A Standards-Based Evaluation of Inverter Technologies: A Case Study for a Hamilton College Solar Farm

Hamilton College Department of Physics

Grace Crowley
Advisor: Charles Collett

Fall 2025

Contents

1 Abstract

As more renewable energy sources replace synchronous generators on the electrical grid, concerns about managing electrical grid stability have grown as current grid operations and controls are based on decades of experience tailored to the physical properties of synchronous machines. Since renewable energy sources are inverter-based resources, grid-following (GFL) inverters were developed to synchronize with the grid, while grid-forming (GFM) inverters were developed to emulate the grid stability provided by synchronous machines. This thesis seeks to evaluate which type of inverter Hamilton College should use if it were to construct a solar farm that directly connects to the school's load while still maintaining its utility grid connection. A model of the Hamilton College system is built on PSCAD and electromagnetic transient (EMT) simulations are run using each inverter type: grid-following (GFL), GFM droop control, GFM virtual synchronous machines, and GFM virtual oscillator controllers. The frequency and voltage results for each inverter were analyzed to determine their compliance with industry standards over an established set of electrical transients. Since the college is still interconnected with the utility grid, the grid dominated the response, with frequency and voltage results for all four inverters staying well within industry compliance levels. GFL inverters are less expensive and involve less maintenance, so it is advised that if Hamilton College were to build this solar farm, it should use GFL inverters.

2 Introduction

2.1 The Electrical Grid

The electrical grid is a critical and complicated piece of infrastructure that is often taken for granted. The grid in the United States undergoes constant monitoring to make sure electricity is constantly delivered to people as needed. When new resources are added to the grid, whether it is conventional gas plant or a solar farm, it must be properly connected to the grid to ensure it is delivering stable power. There are three main categories that dictate power system stability: rotor angle, frequency, and voltage stability [1]. This stability was historically provided by power generators physical machine dynamics [1]. These generators, called synchronous generators, generated power through spinning rotors that converted mechanical energy into electrical energy. Traditional generators' spinning rotor naturally produces alternating current (AC), allowing them to be easily connected to transmission or distribution lines, which carry AC to residential, industrial, or commercial loads.

As renewable energy sources have spread throughout the United States, electrical engineers have had to carefully think about how to connect these new resources to the grid as they contrast starkly with synchronous generators. Renewable resources, such as wind and solar farms, generate direct current (DC). Since the power system was built to support AC, the use of inverters, which convert DC to AC, within the electrical grid has increased to support growing renewable energy. If this conversion is not done, the power produced by renewable energy is less broadly useful and unable to travel on the vast majority of transmission and distribution lines in the United States.

Although these inverters allow renewable energy to deliver AC to the grid, they do not provide the rotor angle, frequency, or voltage stability that synchronous generators do. Instead, inverters use control methods that help to emulate synchronous generators' stability in voltage and frequency, and the inverter phase angle acts as the virtual rotor angle [1]. Phase angle, in this context, is the difference of the instantaneous phase of the voltage to the grid's, and is closely tied to the frequency. If the inverter's control methods are insufficient, these inverters could contribute to grid instability by discharging improper amounts of these quantities. Grid instability can lead to power loss as grid operators work to stabilize critical infrastructure. This can leave people without heat or air conditioning during extreme weather events, threaten their health, or during extended outages, cause perishable food to spoil, costing families money. Furthermore, large variations in frequency can permanently damage grid infrastructure and even everyday electronics that are connected to a wall. This is why it is critical to evaluate the

different types of inverters and control methods that exist for inverters and make sure the right one is selected for interconnection projects.

2.2 Inverter Types

There are two main types of inverter: grid-following (GFL) and grid-forming (GFM), with GFM containing three main control methods: droop control, virtual synchronous machines (VSM), and virtual oscillator controllers (VOC) [1]. GFL inverters are the most traditional and simple inverter, while GFM inverters offer more complex control methods that make them more self-sufficient during grid instability [2]. All three of the GFM inverter control methods produce a similar output that classifies them as GFM, but since they use different methods to achieve this output, there are inherent strengths and weaknesses of each for achieving grid stability. There has been previous research evaluating the difference between these inverters, indicating that GFM inverters are clearly more reliable in isolated systems, but the need for that reliability and the required type of control method depends on the specific use case [1].

2.3 Experiment Objectives

The objective of this thesis is to determine which inverter Hamilton College should use if a solar farm were constructed to connect directly to the campus electrical system while the school remains interconnected with the utility grid. Four inverter types are considered: GFL, GFM droop control, GFM VSM, and GFM VOC. This thesis investigates whether the combined system, consisting of both the solar farm and the utility grid, provides sufficient stability to operate with GFL inverters, potentially avoiding the increased complexity and cost associated with GFM inverters.

3 Theory

3.1 Alternating Current: Electrical Components

In order to understand how inverters function and how GFL inverters differ from GFM inverters, a basic background is needed. As a reminder current (I) is defined as the rate of flow of electrical charge past a point, and voltage (V) is defined as the electric potential difference between two points or the work done to move a unit of positive charge from the more negative point (lower potential) to the more positive point (higher potential) [3].

Since the electrical grid mainly delivers electricity via AC, voltage and current are constantly changing. One way to measure the magnitude of a voltage an AC is waveform is using the root-mean-square (RMS) voltage. RMS voltage is the square root of the mean of squares of the instantaneous voltages over a cycle, which allows for RMS voltage to represent the DC voltage equivalent to the AC voltage [3]. RMS voltage is one common method used to measure voltage in the grid.

Another important topic that arises from AC, is the use of capacitors and inductors. These components are helpful to understanding more complicated topics such as active and reactive power, which will be explained in the next section.

A capacitor is a pair of closely-spaced metal plates, separated by some insulating material, and it stores energy in an electric field between its plates [3]. The relationship between capacitance, current, and voltage is defined as

$$I = C\frac{dv}{dt} \tag{1}$$

, where C is the capacitance in farads [3]. The larger the capacitance, the larger the current needs to be to change the voltage, yielding a core rule in electronics: capacitors resist changes in voltage. This equation also helps explain why a pure capacitor in AC circuits cause the current's phase to lead the voltage by 90° [3]. In an AC system, the voltage will be in the form of a sine wave, and taking the derivative of the voltage sine function results in a cosine wave for the current, which leads a sine wave by 90°. Although in the electrical grid capacitors are far

from the theoretical pure capacitor, so it never causes a full 90° phase difference, understanding that capacitors cause the current to lead the voltage is helpful to understanding reactive power discussed in the next section.

Inductors, on the other hand, store energy in a magnetic field created by current flow through them. The relationship between inductance, current, and voltage is defined by,

$$V = L\frac{dI}{dt} \tag{2}$$

where L is the inductance in henries. The inductor will resist changes in current. In AC, voltage travels in a sine wave form, and following the equation above, current must travel as a negative cosine wave; therefore current is shifted -90°, lagging the voltage [3].

Having both capacitive and inductive elements throughout the electrical grid create a phase shift between the current and voltage. This phase shift, or difference in phase between current and voltage, is called the phase angle.

Other important terminology that arises from the use of inductors and capacitors is impedance (Z) and reactance (X). Inductors and capacitors exhibit reactance, which is their opposition to alternating current (AC) [3]. Impedance represents the combined effect of resistance and reactance in a circuit with both resistive (R) and reactive components, and is defined as:

$$Z = R + jX$$

where $j = \sqrt{-1}$ is the imaginary unit used in phasor analysis to capture the relationship between voltage and current in inductive and capacitive elements [3].

With definitions established for these critical AC circuit components, a formal definition of power in electrical grids can now be introduced.

3.2 Power in AC Systems

There are three different types of power that are present in the electrical grid: apparent power, active power, and reactive power.

Apparent power represents the total power in an AC circuit. Its value can be calculated from

$$S = VI \tag{3}$$

where S is apparent power (in volt-amperes, VA), V is voltage in volts, and I is current in amps [4].

Active power is the form of power most commonly associated with useful work. It powers lights, motors, and electronic devices. It represents the power dissipated by a load and its value is given by,

$$P = VI\cos\phi \tag{4}$$

where P is Active power (in watts, W) and ϕ is the phase angle between voltage and current [4]. Active power is carried by the current component that is in phase with the voltage [5].

In the electrical grid, frequency and active power have a tight relationship [1]. This is a result of the rotational inertia of synchronous machines. Synchronous machines are used at power plants to convert mechanical energy, from a steam turbine or gas turbine, to electrical energy. The machine uses a rotating electromagnet to create a magnetic field that rotates at a constant speed. This magnetic field passes over three stationary coil windings 120° apart, which create a balanced three-phase AC power as the rotor spins.

When the load of the system increases the spinning turbine cannot immediately produce more power because of its inertia, instead the turbine will spin slower as power is pulled into the load [1]. The decreased rotation of the turbine will lower the frequency. This means that any active power imbalance speeds up or slows down the generators rotors, changing the frequency. Consequently, managing active power is fundamental to maintaining frequency stability in AC power systems.

Reactive power, on the other hand, is the power absorbed and released by inductive or capacitive elements due to their reactive properties and is given by,

$$Q = VI \sin \phi \tag{5}$$

where Q is reactive power (in volt-ampere reactive, VAR) [4]. Reactive power is not consumed by the load but instead supports voltage and maintains electric fields. To put it another way, reactive power is created from current flowing through reactive components and affects voltage levels but does not transfer any net energy.

Reactive power is needed wherever there are inductive or capacitive elements in the grid, such as transmission lines, transformers, and motors, which store and release energy in their magnetic or electric fields each AC cycle [1]. These components create network reactance that cause the current to lag (for inductors) or lead (for capacitors) the voltage, producing a nonzero phase angle (ϕ) between the voltage and current as explained in the previous section. A helpful rule of thumb is that inductive loads, such as motors and transformers, absorb reactive power, while capacitive elements produce it [4].

As active power is linked to frequency, reactive power primarily affects voltage [1]. When a load draws more reactive power, it draws additional reactive current. This current flows through the network reactance, producing a voltage change: inductive reactance causes a voltage drop, while capacitive reactance produces a voltage rise. During a drop in voltage, even if generators or inverters supply the additional reactive power, the voltage still settles slightly below the nominal value because current must flow through the network's inductive reactance [1]. Therefore, managing reactive power is fundamental for maintaining voltage stability in AC power systems.

These three types of power form what's known as the power triangle, with apparent power (S) as the hypotenuse, as illustrated in Figure 1.

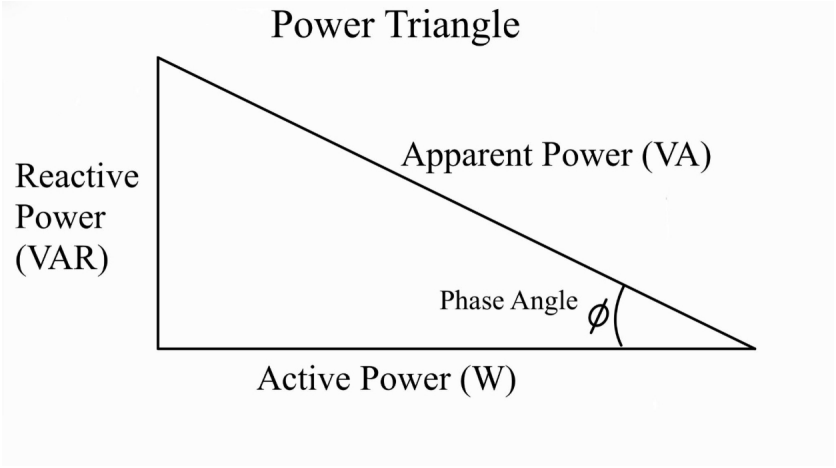

Figure 1: Power triangle depicting the relationship between active, reactive, and apparent power. The phase angle is the difference in phase between the current and voltage.

Another helpful definition related to the power triangle is power factor. Power factor (PF) is the effect of the load on the AC phase and ranges from 0 to 1. If the PF is 1, the load is purely resistive with no phase shift. If the PF is 0, it's a purely reactive load and no net current flows [4]. It is mathematically defined as the ratio of P to S or $PF = \frac{P}{S}$.

Although GFM and GFL inverters are not generating power or directly changing active or reactive power, the inverter's role in controlling the current and voltage output affects the active and reactive power output to the grid. The close relationships also mean that active or reactive power is used within control logic to then manage voltage and frequency stability. Understanding active and reactive power is key to fully understanding the control logic used in GFL and GFM inverters.

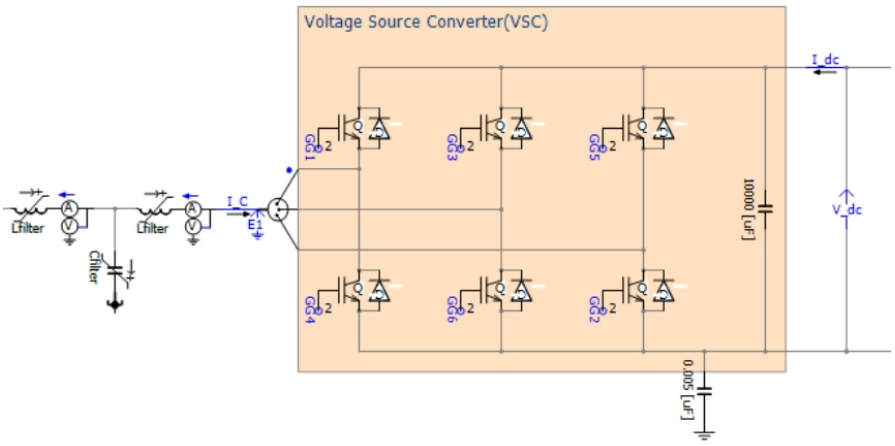

Figure 2: Imagery of PSCAD simulation inverter clearly showing the 6 different switches as well as the LCL filter on the left hand side [6].

3.3 Inverters

It is important to have a base knowledge of how inverters work before delving into GFL or GFM inverters that have added control components. A three-phase inverter, the type of inverter used in this experiment is composed of six different switches and a smoothing filter. The specific type used in this model is insulated gate bipolar transistors (IGBTs) [6]. An IGBT is a switching device that requires almost no steady input current to control it, yet can efficiently handle and regulate large power flows. This combination makes it ideal for inverters, where it rapidly switches DC on and off to create precise AC waveforms with high efficiency and minimal control power [3].

These switches allows current to flow when a voltage is applied to the gate. The six switches are arranged in two rows of three as shown in figure 2. The switches are turned on at precisely the right time so that the output is either the higher current on the top bar, or the lower current on the bottom bar. This switching causes the DC to take a square wave form that is smoothed into a sine curve with an Inductor-Capacitor-Inductor (LCL) filter, shown on left hand side of figure 2. How each type of inverter uses the current and voltage measurements from the grid to calculate its power output, defines them as GFL, GFM droop control, GFM VSM, or GFM VOC, and results in different levels of grid stability. In order to actually inject power into the grid, the inverter needs to deliver a small phase lead at the point of common coupling (PCC), where the inverter connects to the grid. If the phase angle of the inverter is greater than that of the grid, then the inverter will inject power.

3.4 Important Reference Frame Definitions

Before defining any control methods, it is important to note the frame transformation that the three-phase AC goes through from the natural abc frame into rotating reference frames, the DQ frame and dq frame. These reference frame transformations simplify inverter control by converting the oscillatory three-phase AC quantities into slowly varying or constant signals. The rotating reference frames are also helpful since they allow for the active and reactive power components to be largely decoupled, enabling independent regulation.

The first step, the abc–DQ transformation, converts the three-phase signals into a synchronous frame rotating at the nominal grid frequency ($60Hz * 2\pi$ rad/s), the DQ frame. A second rotation, from DQ to dq, aligns these quantities with a reference frame that may rotate at any angular velocity or remain stationary, commonly referred to as the arbitrary reference frame [7]. The dq or DQ frame, depending on angular velocity being used, can be used to decouple the current into its d-axis component (real current, Id, also named Ip component) and the q-axis, the reactive current component, Iq [5]. This allows the independent regulation mentioned

earlier, with Ip controlling the real power output, and Iq controlling the reactive power output [5].

Note that within the simulation, ABC to DQ frame blocks use ϕ, not the nominal grid frequency ($60Hz * 2\pi$ rad/s) for the phase transformation. This reference frame transformation is more similar to what would be abc-dq transformation, as the three-phase signals match to an arbitrary angular velocity, ϕ. The DQ frame is only seen in theory, not the actual simulation, but is critical to understand for the mathematical theory of GFM inverters.

3.5 Phase Locked Loops

Certain inverters use a phase-locked loop (PLL) to match the inverter output frequency to the grid. A PLL uses an oscillator to adjust the inverter's output phase and frequency to match what it is reading from the grid voltage and will force the output to 'lock' to the grid's phase and frequency [1]. A PLL contains a phase detector, amplifier, and voltage-controlled oscillator (VCO). The phase detector is a device that compares two input frequencies and outputs the difference in those frequencies. The two input frequencies are f_{in}, measured from the grid, and f_{VCO}, the PLL's internal frequency. If f_{in} doesn't equal the f_{VCO}, after it has been filtered and amplified, the VCO frequency will deviate in the direction of f_{in}. If the difference in frequencies is zero, $f_{in} = f_{VCO}$ the VCO will quickly "lock" to f_{in}, maintaining a fixed phase relationship with the input signal [3].

3.6 Grid Following Inverters

Grid following (GFL) inverters function through 'reading' the voltage and current of the electrical grid and setting the correct angle and phase of current to output. Controlling the output current is what allows the GFL inverter to inject or absorb the proper amounts of active or reactive power so the grid remains stable [1]. This is where the 'following' name comes from. These inverters will follow what the grid is telling it to do because GFL inverters do not have the capability to set an internal voltage. Most GFL inverters use a Phase Lock Loop (PLL) to match the current to what it is reading from the grid [1].

Literature does not clearly define equations for GFL control that are helpful to compare with GFM control equations, which will be introduced in the next section. Instead, defining how the GFL inverter controls frequency and voltage in the PSCAD simulation will help show how GFL inverters differ from GFM inverters.

3.6.1 Simulation of GFL Inverters: Frequency, Phase Angle, and Current Control

Within the simulation the difference between GFL inverters and GFM inverters lies in the outer controls and synchronization block. This block takes two input variables, the voltage and current from the grid, and outputs "Id-ref", the real current component in the dq frame, "Iq-ref", the reactive current component in the dq frame, "freq-control", the instantaneous frequency (ω), and "phi", the instantaneous phase angle (ϕ). The control block is shown in Figure 3.

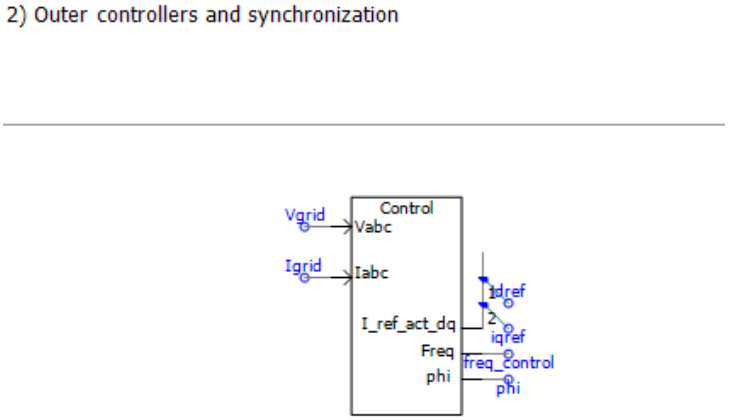

Figure 3: Visual of the input and output of the controls and synchronization block in the PSCAD model. The controls executed in this block are what differentiate each type of inverter.

How the simulation calculates and uses ω and ϕ while in GFL mode helps in understanding how GFL inverters control frequency and phase angle. Similarly, how the simulation calculates and uses Id-ref and Iq-ref while in GFL mode helps in understanding how GFL inverters control current.

Using a PLL for Frequency and Phase Angle Control:

Within the outer controls and synchronization block, GFL inverters use a PLL to calculate both ϕ, instantaneous phase angle, and $\omega(t)$, instantaneous frequency, from the measured grid voltage. This means that ϕ, used for reference frame transformation, will align with the external grid. Similarly, the frequency of the inverter output, is calculated from a PLL, making ω grid-aligned as well.

For context, the phase angle ϕ is used directly in the abc–dq transformations to define the instantaneous orientation of the rotating reference frame. ϕ is also used to transform the real voltage component (Vd) and reactive voltage (Vq) component, which are calculated from Id-ref and Iq-ref, into three voltages in the abc reference frame. These three voltages then create the six firing pulses that control the six switches in the inverter. The frequency measured from the PLL is used to calculate Ipvd-ref, which will be describe in more detail in the following current control explanation.

Using P and Q for Current Control:

During the simulation Ipvd-ref is generated by active power control loops, and Ipvq-ref is generated by reactive power control loops. The inverter measures grid voltage and current to compute real and reactive power (Pelec and Qelec), and uses the difference between the reference power and measured power, Pref − Pelec, to produce the d-axis (real current) current reference, and Qref − Qelec to produce and q-axis (reactive current) current reference.

The inverter is only using power errors to determine how much current to inject into the grid. Although the inverter measures voltage, it does not directly regulate voltage. As a result, the GFL inverter lacks the authority to set or restore grid voltage levels and can only adjust its own current injection.

Id-ref and Iq-ref are then used to get real voltage component and reactive voltage component. These voltage commands are transformed back into the abc frame and used to produce the six switching signals that control the inverter output. The power tracking used to control the current, Id-ref and Iq-ref, is a key differentiator between GFL and GFM inverters.

3.7 Grid Forming Inverters

The essential difference between grid-forming and grid-following inverters lies in their control objectives. Grid-forming inverters operate as voltage sources capable of establishing and regu-

lating their own terminal voltage because they do not need a grid reference to operate. Voltage sources are defined as two-terminal "black boxes" that maintain a fixed voltage drop across their terminals [3]. In contrast, grid-following inverters act as current sources, injecting current to match an existing grid voltage [1]. Current sources are defined as two-terminal black boxes that maintain a constant current through the external circuit [3]. Because GFM inverters can generate their own voltage reference, they are particularly effective in black-start scenarios, where they can energize a de-energized network.

Another important aspect of GFM inverters is their dependent relationship between frequency and active power, as well as voltage and reactive power. GFM inverters emulate this P-ω and Q-V coupling through control algorithms that adjust frequency in response to active power changes and voltage in response to reactive power changes. This behavior allows multiple GFM inverters to synchronize with one another, with each device contributing a proportional share of active and reactive power while still maintaining overall frequency and voltage stability [1].

3.7.1 Mathematical Theory for GFM Inverters

With these properties, GFM inverters relate their terminal voltage and frequency to the active and reactive power exchanged with the grid. The generalized equations used for the active (p) and reactive power (q) output of GFM inverters are,

$$p(t) = e^*(t)e_1^\top T_2(\delta(t))T_1(\omega_0 t)i_i(t) \tag{6}$$

$$q(t) = e^*(t)e_1^\top T_2\Big(\delta(t) - \frac{\pi}{2}\Big)T_1(\omega_0 t)i_i(t) \tag{7}$$

[7]. Where: $e^*(t)$ is the reference voltage magnitude of the inverter at time t,e_1 is the 2×1 standard basis vector $[1\ 0]^\top$, $T_1()$ is the abc-to-DQ transformation matrix, $T_2()$ is the DQ-to-dq rotation matrix, $\delta(t)$ is the phase-angle deviation from the nominal frame, ω_0 is the nominal angular frequency (e.g., $2\pi 60$ rad/s), $i_i(t)$ is the inverter-side current vector of the LCL filter.

$e^*(t)$ and ω are defined differently depending on the type of control method used in the GFM inverter. Note, $\delta(t)$ changes with respect to ω. Three primary control methods for grid-forming (GFM) inverters are widely recognized: droop control, VSM, and VOC.

Droop Control:

Droop control emulates the steady-state behavior of synchronous generators by linearly relating frequency and voltage magnitude to deviations in active and reactive power, reflecting the relationship between voltage and reactive power and frequency and active power that was discussed in the Theory. This approach enables autonomous power sharing among parallel inverters without communication, another key characteristic of GFM inverters. Droop control qualifies as grid-forming because it directly establishes voltage and frequency references, unlike a GFL inverter that tracks an external grid signal [7]. The equations used to find the reference voltage, e^*, and the angular frequency ω, in droop control are,

$$\omega = \omega_0 + \frac{1}{d_f}e_1^\top T_2\Big(\psi - \frac{\pi}{2}\Big)\begin{bmatrix}p^* - p_m\\ q^* - q_m\end{bmatrix} \tag{8}$$

$$e^* = e_0 + \frac{1}{d_v}e_2^\top T_2\Big(\psi - \frac{\pi}{2}\Big)\begin{bmatrix}p^* - p_m\\ q^* - q_m\end{bmatrix} \tag{9}$$

where ω is instantaneous inverter angular frequency (rad/s), ω_0 : Nominal angular frequency (e.g., $2\pi \times 60$ rad/s), d_f is the frequency droop coefficient, d_v is the voltage droop coefficient, e_0 is the nominal voltage magnitude (per unit), e_2 is a 2×1 standard basis vector [0; 1], ψ: is the rotation angle determining coupling between active/reactive power and frequency/voltage, p_m, q_m are the measured active and reactive power outputs of the inverter, and p^*, q^* are the reference (set-point) active and reactive power outputs [7].

These equations show how droop control uses specific droop coefficients, d_f and d_v, to control both frequency and voltage. It is also calculating the difference between the reference active and

reactive power versus their measured values, showing the control adjusting to any deviation from the grid.

Although equations 8 and 9 capture how droop control functions, adjusting frequency and voltage in response to active and reactive power deviations, these are theoretical expressions rather than practical implementation formulas. As defined earlier, a GFM inverter, does not 'read' the grid, despite these equations using p_m and q_m. The equations are primarily used to illustrate droop control concept and to provide a clear mathematical framework for understanding how frequency and voltage respond to power imbalances. A similar rule follows for equations 10 and 11, which also use q_m.

Virtual Synchronous Machines: VSM control extends droop control by introducing virtual inertia, m_f, and damping, d_d, to mimic the electromechanical swing dynamics of a synchronous generator. By adding inertia and damping, VSMs provide frequency support and smooth dynamic behavior during transients. Like droop control, the VSM defines its own voltage and frequency internally and is therefore grid-forming [7]. Its equations for ω and e^* are defined as,

$$\omega = -\frac{m_f}{d_f}\dot{\omega} + \omega_0 + \frac{d_d}{d_f}(k_P\dot{\eta} + \omega_0 k_I \eta) + \frac{1}{d_f}e_1^\top T_2\Big(\psi - \frac{\pi}{2}\Big)\begin{bmatrix} p^* - p \\ q^* - q_m \end{bmatrix} \tag{10}$$

$$e^* = e_0 + \frac{1}{d_v}e_2^\top T_2\Big(\psi - \frac{\pi}{2}\Big)\begin{bmatrix} p^* - p \\ q^* - q_m \end{bmatrix} \tag{11}$$

where m_f is the virtual inertia constant, d_d is the damping coefficient, and (k_P, k_I) are the proportional and integral gains of the phase-locked loop (PLL). The variables $\eta(t)$ and $\alpha(t)$ denote the internal state and output phase of the PLL, respectively. The PLL estimates the grid frequency as $\dot{\alpha}(t) = k_P\dot{\eta}(t) + k_I\eta(t)$ and provides this information for synchronization within the VSM control loop [7].

It is important to note PLL values appear in theory because they provide the mathematical way to estimate the grid's phase and frequency, even though a VSM does not use a PLL to control its own dq frame.

Virtual Oscillator Controllers:

Virtual oscillator controllers (VOC) models the inverter as a self-synchronizing nonlinear oscillator whose internal voltage state naturally aligns in phase and amplitude with the grid while its natural frequency matches the nominal grid frequency [1]. The VOC approach achieves grid-forming behavior through nonlinear self-synchronization rather than explicit droop laws or external phase tracking. Frequency and voltage emerge as properties of the oscillator dynamics [7]. The equations used to define ω and e^* are,

$$\omega = \omega_0 + \frac{\omega_0\kappa_1}{(e^*)^2}e_1^\top T_2\Big(\psi - \frac{\pi}{2}\Big)\begin{bmatrix} p^* - p \\ q^* - q \end{bmatrix} \tag{12}$$

$$\frac{1}{\omega_0\kappa_2}\dot{e}^* = -(e^*)^3 + e_0^2 e^* + \frac{\kappa_1}{\kappa_2 e^*}e_2^\top T_2\Big(\psi - \frac{\pi}{2}\Big)\begin{bmatrix} p^* - p \\ q^* - q \end{bmatrix} \tag{13}$$

where κ_1 is the synchronization gain that denotes the coupling between the inverter's frequency and power deviations, and κ_2 is the voltage-amplitude control gain that regulates the magnitude dynamics of the inverter's terminal voltage. These gains define the dynamic behavior of the VOC in coordinating voltage and frequency regulation [7].

Clarifying the application of the $P + \omega$ and $Q + V$ relationships:

Across the three different control methods both equations for ω and $e*$, equations 6 to 13, use both p and q deviations despite the coupling in power systems linking active power to frequency and reactive power to voltage. It is common for modern grid-forming inverter controls to include cross-coupling between P and Q within the frequency and voltage control. They are used to compensate for inverter dynamics, improve stability, and ensure synchronization under disturbances. As a result, the GFM control equations often take a matrix form in which both active and reactive power deviations contribute to the updates of the internal frequency and voltage reference [7].

3.7.2 Simulation of GFM Inverters: Frequency, Phase Angle, and Current Control

As described in Section 3.6.1, within the simulation the difference between GFL inverters and GFM inverters lies in the outer controls and synchronization block, see Figure 3. This block takes two input variables, the voltage and current from the grid, and outputs "Id-ref", the real current component in the dq frame, "Iq-ref", the reactive current component in the dq frame, "freq-control", the instantaneous frequency (ω), and "phi", the instantaneous phase angle (ϕ).

How the simulation calculates and uses ω and ϕ while in each GFM mode helps in understanding how different GFM inverters control frequency and phase angle. Similarly, how the simulation calculates and uses Id-ref and Iq-ref while in each GFM mode helps in understanding how different GFM inverters control current.

Using Active Power for Frequency and Phase Angle Control

Within the simulation both GFM droop control and GFM VOC inverters do not use a PLL to calculate ω or ϕ. These inverters rely on $Perr$, the filtered and limited active power imbalance signal produced by a measurement transducer. Their frequency is directly determined from active power error through the enforced P-ω relationship, and the phase angle is obtained by integrating the internally generated frequency.

VSM includes a PLL to measure grid voltage angle and frequency, but this PLL does not dictate the inverter's frequency. Instead, the inverter frequency evolves according to the swing equation, with the PLL serving only as a measurement and reference aid for power calculation.

In all three GFM inverter modes the calculated frequency is used to continuously calculate $Perr$ and $Qerr$. Similar to in GFL mode, when in GFM mode the phase angle ϕ is used in the abc–dq transformations to define the instantaneous orientation of the rotating reference frame. ϕ is also used to transform the real voltage component (Vd) and reactive voltage component (Vq), which are calculated from Id-ref and Iq-ref, to three voltages in the abc reference frame. These three voltages then create the six firing pulses that control the six switches in the inverter.

Using Voltage for Current Control

In the GFM inverter, Ipvd-ref and Ipvq-ref are produced by voltage-regulation loops, not power-regulation loops. The inverter creates its own internal voltage reference, E_{ref}, or e^* as defined in equations 9, 11, and 13 for the d-axis reference voltage. Although in equations 9, 11, and 13 e^* is calculated using both p and q, within the simulation only q is used, which aligns with the Q-V relationship GFM inverters enforce. Vq-ref is used for the q-axis reference voltage.

Vpvd is the d-axis voltage from the solar farm (hence the 'PV' in the variable), and Vpvq is the q-axis voltage. The d-axis and q-axis voltage errors ($E_{ref}-$ Vpvd) and (Vq-ref $-$ Vpvq) are used to generate the required current commands for the inner current controllers, calculating Ipvd-ref and Ipvq-ref, which are renamed to Id-ref and Iq-ref once outputted from the outer controls and synchronization block. Because these commands originate from voltage control, not power tracking, the GFM inverter behaves as a voltage source capable of establishing and maintaining grid voltage and frequency, which is why GFM control enables black-start-capable operation.

As clarified in past sections, the Id-ref and Iq-ref variables are used to find real voltage component and reactive voltage component. These voltages are transformed back into the abc frame and used to produce the six switching signals that control the inverter output. The voltage regulation used to control the current, Id-ref and Iq-ref, is a key differentiator between GFL and GFM inverters.

4 Methods

The goals of this thesis are to adapt an existing PSCAD model to represent the Hamilton College electrical system and its solar farm, and to use this model to run electromagnetic transient (EMT) simulations. These simulations are used to evaluate which inverter type is best suited for Hamilton College's solar farm. Specifically, the inverter responses to three transient events are analyzed. Voltage and frequency behavior during each transient is compared against established industry standards to assess whether each inverter can provide stable and reliable power to the Hamilton College grid.

This experiment is conducted through simulation using PSCAD [8]. PSCAD is an advanced software for EMT simulations of power systems. EMT simulations show how certain models of electrical systems respond to different transients, which are short-term disturbances to voltage or current. These transients are often triggered by factors such as the switching operations of inverters (rapid exchange of energy between inductive and capacitive elements in a network) that can result in excess voltage or current, potentially damaging equipment or harming grid system stability. In an EMT simulation, PSCAD numerically solves the time-domain differential and algebraic equations of all system components, such as sources, loads, transmission lines, power electronic devices, simultaneously at each simulation time step. Electrical components can be modeled with differential equations because their behavior is based on the change of electric and magnetic fields over time, for example equations 1 and 2 store energy and introduce time derivatives of voltage and current.

PSCAD can capture fast electromagnetic and control-driven events, such as switching behavior, fault transients, and inverter dynamics, that occur on microsecond to millisecond timescales [8]. Because of this detailed time-domain modeling capability, PSCAD is well suited for evaluating inverter-based resources and their impact on network stability. Other power system simulation tools are typically designed for power-flow analysis or phasor-domain dynamic simulations, which operate on slower timescales and are more appropriate for studying steady-state conditions or electromechanical dynamics rather than high-frequency transients.

4.1 Original Generalized PSCAD Model

The new Hamilton College model is based off an existing GFM and GFL inverter model [2]. This original model was intended to investigate how different types of inverters interact with one another and contribute to overall system stability. With the increasing penetration of renewable energy and inverter-based resources, the goal of this model is to examine inverter operation in a network without synchronous machines [2].

This model's topology consisted of a solar farm connected to a general system that included a basic fixed load, which was connected to a second solar farm on the other side of the fixed load as shown in figure 4. Figure 5 shows a detailed view of the solar farm, labeled 'PVFarm GFL-GFM' in Figure 4. The system, labeled 'Sys' in Figure 4, includes the load, labeled 'P+jQ', along with three different multimeters, labeled Bus 1, Bus 2, and Bus 3 as shown in Figure 6. The three buses measure voltage, active power, reactive power, and frequency measurements every 50 μs. These measurements are graphed over a ten second period and used to analyze the stability of the system.

The three transients used are a 10% increase in load released at 3 seconds, a three-phase fault to ground at 5 seconds, and another increase in load at 7 seconds. The transient logic is shown in Figure 6: the two load increases are located below the two red breaker load blocks, which release the load at the assigned time, and the three-phase ground to fault is on the left hand side (ABC $\rightarrow$ G). A fault is when current accidentally travels through a low-impedance return path. A return path is when current is returning back to the source after a load has drawn power from the AC. Instead of its typical high-impedance path back through long transmission or distribution lines, something (named the fault), creates a new unintended connection between two of the three phase wires, and current flows through that connection because it has much lower impedance. This new path causes large currents and a collapse in voltage until the fault ends. These transients are used to evaluate how the Hamilton College model complies with industry standards for voltage and frequency as laid out in the next section.

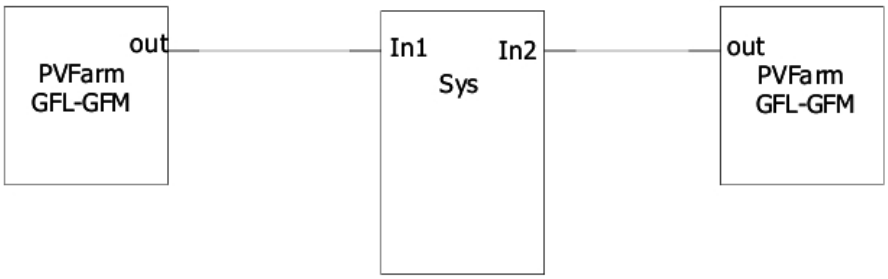

Figure 4: Original topology of the two solar farm system. Each PVFarm can be designated to be either a GFL, GFM droop control, GFM VSM, or GFM VOC inverter [2].

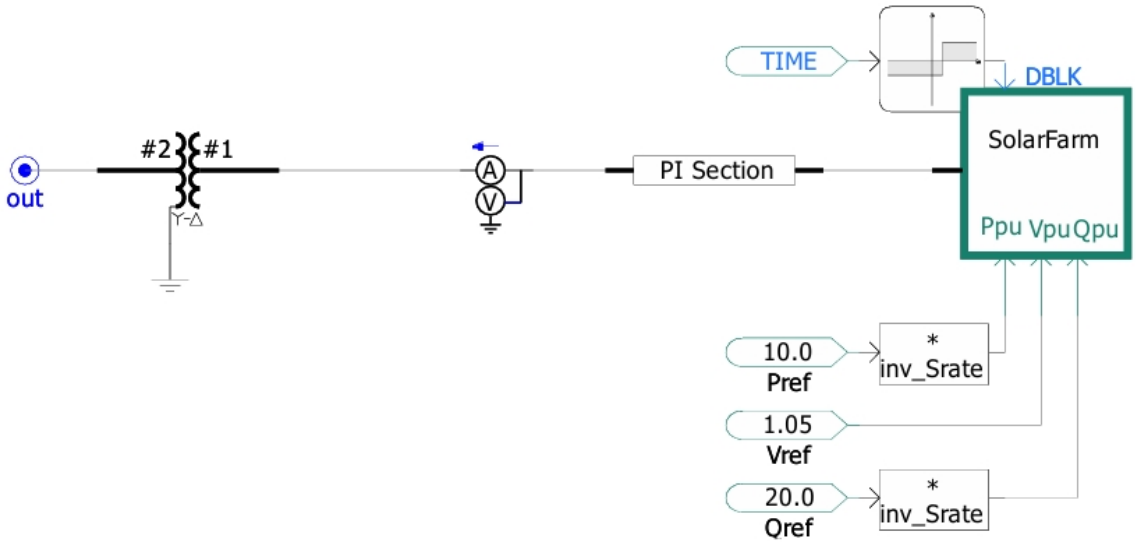

Figure 5: View of the PVFarm with designated references for active power (P), voltage (V), and reactive power(Q) [2].

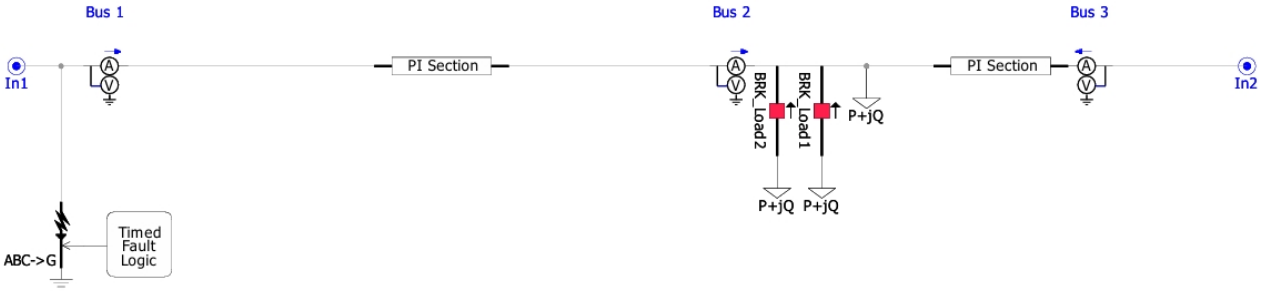

Figure 6: Detailed view of 'Sys', which includes the main fixed load, the rightmost labeled $'P + jQ'$, the two additional loads, 10% the size of the main fixed load, released at 3 seconds and 7 seconds, respectively, labeled as 'BRK_Load1' and 'BRK_Load2'. The main fixed load is adjusted to reflect the size of Hamilton College's load. Timed fault logic for three-phase voltage to ground is shown on left hand side. [2].

4.2 General Industry Standards

These simulations will show how the different inverters respond to increasing load and voltage instabilities, helping to demonstrate which inverter would be the most resilient in supplying Hamilton College with energy. These transients are standardized and used in existing literature to test system stability, such as large solar farm installations [2]. The general industry standards for voltage and frequency stability in the Eastern Interconnection of North America, where Hamilton College is located, are shown in Figures 7 and 8. The results of different inverters will be compared against each other to evaluate stability while also making sure voltage and frequency levels stay within the 'No Trip Zone'. It is a possibility that a GFL inverter, although typically less stable than a GFM inverter, is stable enough and within industry standards, saving the college the time and money the GFM inverters require.

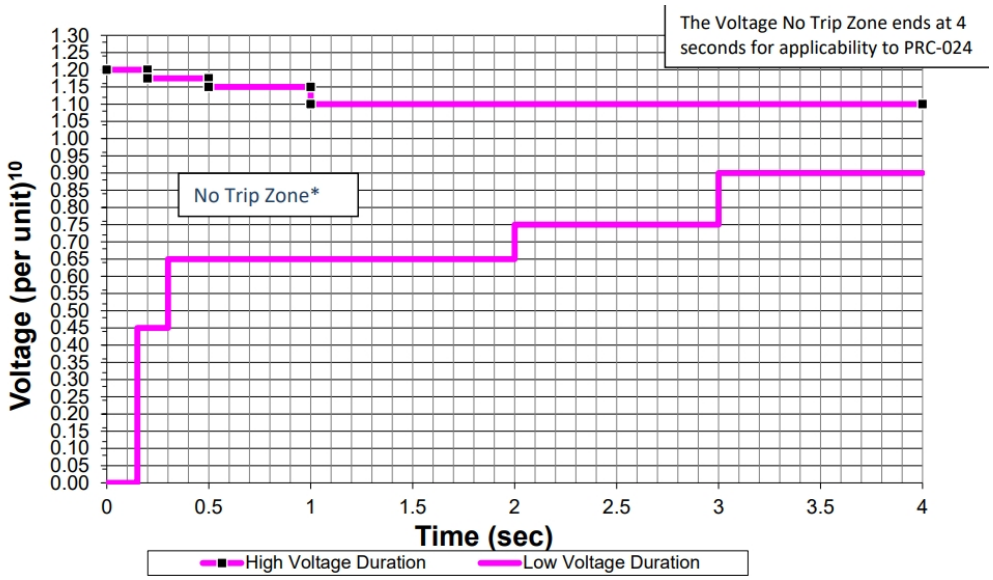

Figure 7: The 'No-Trip' zone shows the voltage level constraints for the Eastern Interconnection, where Hamilton College is located. Specifies what voltage levels the load can safely operate at over a certain period of time taken from [9].

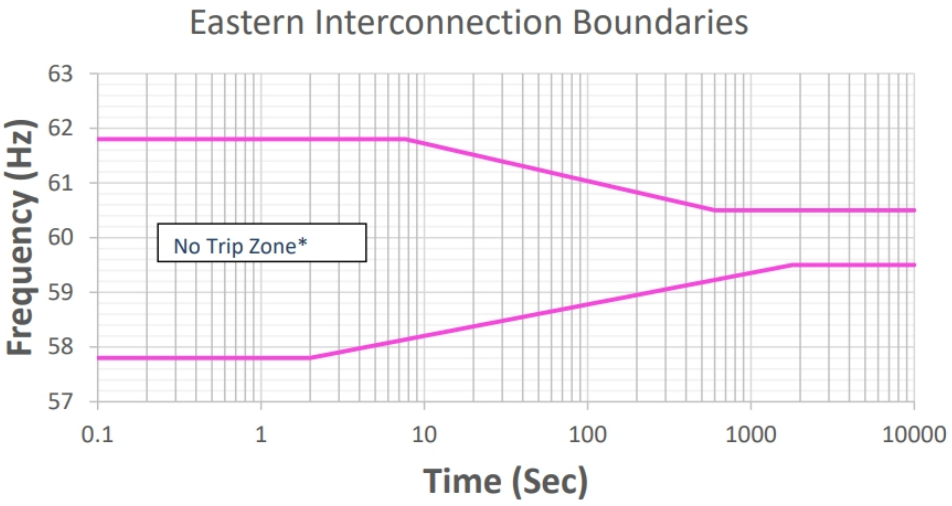

Figure 8: The 'No-Trip' zone shows the frequency level that the Hamilton College load can safely operate at over a certain period of time [9].

4.3 Creating the Hamilton College Model

In order to simulate a Hamilton College solar farm, both the fixed load values and the solar farm values had to be adjusted. Also, one of the solar farms had to be replaced with an energy source to simulate the electrical grid that Hamilton is connected to.

4.3.1 System changes

Starting with the major changes that happened to the system, the fixed load was changed to be the size of Hamilton College's load. Using information from the college's facilities, the fixed load was set to a peak amount of 3.6 MW or 1.2 MW per phase, reflecting the amount of power used on a hot summer day. To find the reactive power, the power factor of the load was calculated with the active and reactive power values from the original simulation, yielding a power factor of 0.9738. This power factor and the relationship established between active and reactive power in the power triangle, see Figure 1, was used to find the reactive power of the load. The two increases in load were set at 10% of the new load power values. These changes to the system are laid out in table 1.

Modeling the school as a fixed load is not entirely accurate, as the exact amount of power that the college is using is not fixed, but for a 10-second-long-simulation at this level of analysis, is sufficient. A power factor of 0.97 is high, but also not completely unrealistic given the size of Hamilton College and the potential that some buildings could have power factor correction systems.

Variable	New Model	Original Model
Active Power per phase (MW)	1.2	30
Reactive power (MVAR)	0.28	7
Rated Load Voltage (RMS L-G)	7.62102 kV	69.28 kV
Base Voltage (kV)	13.2kV	120kV

Table 1: Table of values changed for fixed load as well as the new base voltage used in the system.

4.3.2 Solar Farm Changes

The amount of power generated from the solar farm was reduced to a reasonable scale given the size of land available to the college. The school is in the process of planning a land lease solar farm. The details from the proposed land lease solar farm were used to make adjustments to the model. This included the general size of the farm, the number of inverters used, the rated power of the solar farm, and the estimated power factor [10]. Details of the land lease solar farm are laid out in Appendix A. These values were used to directly adjust variables in the solar farm, and, with the use of the power triangle shown in Figure 1, were also used to calculate other variables, such as the Active Power Ref and Reactive Power Ref in Table 2. Since the load of Hamilton College was set to the typical power on a hot day, the solar farm was producing a similar amount of power that it would on a sunny day.

The main difference from this land lease plan compared to this simulation is that the land lease solar farm is connected to the grid, instead of directly feeding into Hamilton College. Also, due to technical difficulties, and concerning simulation results, the solar farm was scaled down even further from the 20 inverter unit solar farm in land lease plans, to a 10 inverter unit solar farm. The 20 unit solar farm supplied more power than the Hamilton College load was using, creating some negative active power results. Without a clear understanding of the implication of this negative active power, the solar farm was scaled down to negate this issue. This adjustment will be further discussed in the Discussion section as potential next steps are laid out.

Table 2 shows key values that were changed from the original general model to the Hamilton College model within the solar farm. It is important to note that there were a plethora of hard-coded values, mainly voltage base values, that had to be manually changed to match those shown in table 2. These hard coded values were found within multimeters, distribution lines (labeled 'PI Section' in Figure 6), transformers, and the three-phase voltage source (shown in Figure 9).

Variable	New Model	Original Model
Rated MW per unit	0.25	0.25
Number of units	10	400
Base Voltage (kV)	0.6	33
Active Power Ref (MW)	2.43	80
Reactive Power Ref (MVAR)	0.608	20

Table 2: Table of Solar farm values

4.3.3 New Electrical Grid Source

A solar farm from the original simulation was replaced with a three-phase voltage source as shown in Figure 9. As a stable source of voltage, this component has been used in other literature to simulate the electrical grid [11]. This is under the assumption the electric grid is functioning as it is supposed to.

Hamilton College has an on-campus substation. This substation steps down 46kV to 13.2kV to be distributed across campus, where each building has its own smaller transformer that steps the voltage down to a typical residential or commercial level. The school has two transformers, each rated at 7.5 MVA. This substation is generalized to one three-phase transformer, rated 15 MVA, to step the voltage down to 13.2kV to deliver it to the fixed load, Hamilton College.

A multimeter was also added to measure active power, reactive power, and voltage. The graphs made from these variables are used to analyze the performance of the different inverters, but in this case are used to double-check the voltage source is functioning as a constant and stable source of power and voltage to the system. This was a helpful quality control check when building out the electrical grid source.

As the standard in North America, the frequency was set to 60 Hz. Also, the reference voltage was set to 1.05 per unit (PU) , which is common practice in PSCAD simulations and was done for both original solar farms [6]. PU voltage is calculated by dividing the measured voltage by a chosen voltage base value. The base value for the multimeter shown in Figure 9, is

46.0kV. The base voltage used at bus 1, bus 2, and bus 3 in the system, see Figure 6, is 13.2kV as given in table 1.

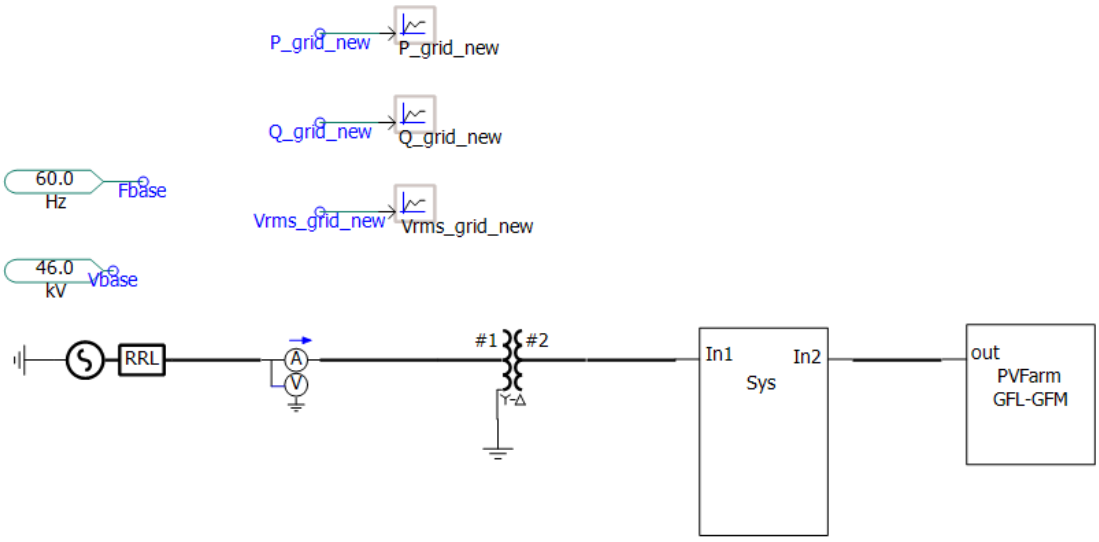

Figure 9: High level view of the whole model with the new voltage source acting as the electrical grid on the left hand side. The electricity then travels through a multimeter, which measures active power, reactive power, and voltage, before reaching the transformer. The transformer steps down the voltage from 46kV to 13.2kV before it travels to the system, labeled "Sys", that contains the Hamilton College load. The solar farm, labeled "PVFarm", provides power on the other side of the system. Note changes from Figure 4.

To quality-control changes made to the mode results of the updated simulation were compared with results from the original simulation. Obviously, the results between the original model and the Hamilton College model will be significantly different, but using the original results helps to make sure changes to the new Hamilton College model are correct, and not giving inaccurate results due to mistakes in the model edits.

4.4 Running the Simulation

Once the new model of Hamilton College was built, simulations for each type of inverter could be run. Setting the solar farm to have GFL, GFM droop control, GFM VSM, or GFM VOC inverters was a straightforward process. Since the inverter controls were built out in the original model, three variables within the parameters of the solar farm designated what kind of inverter control was applied. The three variables are: Q Flag, V flag, and W evaluation type, as boxed in Figure 10. A drop down menu, the "W evaluation type" variable, within the solar farm allowed for inverter designation as SRF-PLL, Droop, VSM, or VOC. By defining the three variables, the inverter type as GFL, GFM droop control, GFM VSM, or GFM VOC with the variables laid out in Table 3.

Inverter Type	Q flag	V flag	W evaluation type
GFL	0 or 1	1	SRF-PLL
GFM Droop Control	1	0	Droop
GFM VSM	1	0	VSM
GFM VOC	1	0	VOC

Table 3: Variable designation for each inverter type in the simulation.

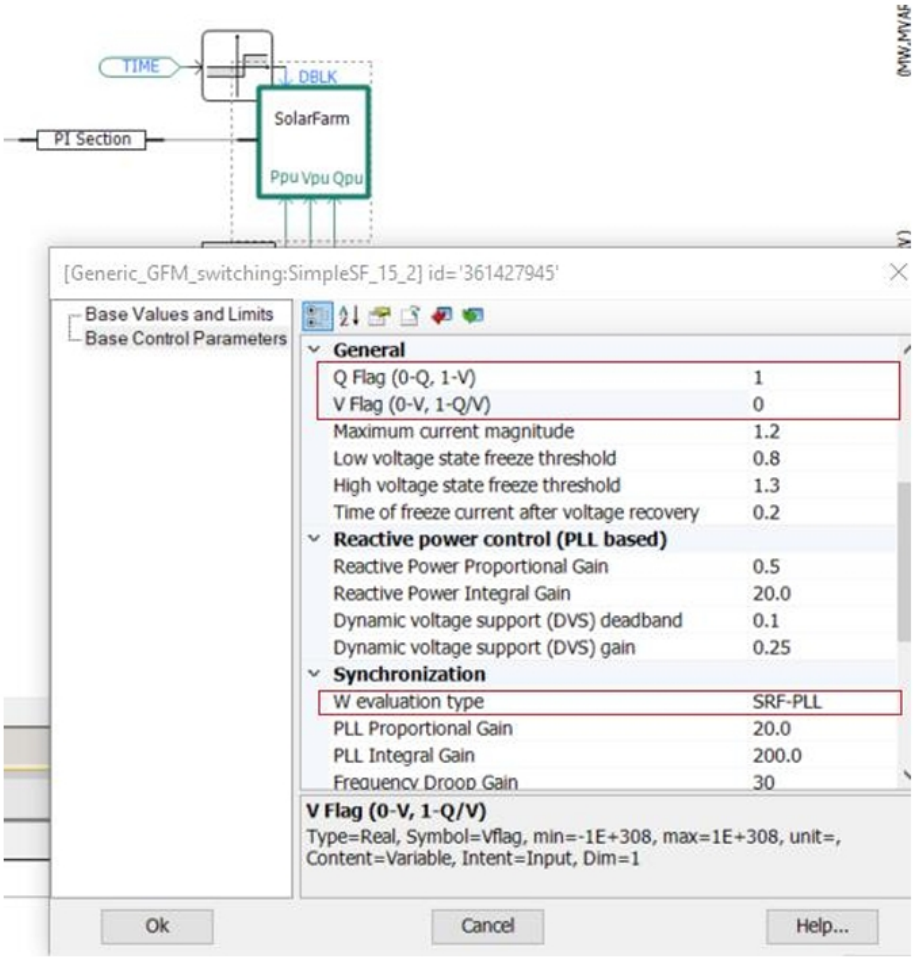

Figure 10: Parameter menu within the SolarFarm component that is shown in Figure 5. The boxed values highlight what variables need to be changed to set what inverter type is used.

During the simulation the software measures and makes graphs of the voltage, frequency, current, active power, reactive power, apparent power, etc at each layer of the model. After each simulation run, there are a lot of graphs providing information about the system stability and solar farm output. For the purposes of this experiment, the graphs that were analyzed were the graphs of voltage, active power, reactive power, apparent power, and frequency at each of the three buses in the system. The labeled buses and system are shown in Figure 6. This is because the system is where Hamilton College, the load, is located and the goal of this experiment is to evaluate the stability of the power provided to the school. Once the simulation is done running, these graphs can be zoomed in on certain times during the simulation to make more detailed analyses. This was done at 3 seconds, 5 seconds, and 7 seconds to get a better view of how the voltage and frequency reacted to the transients at these times. Voltage and frequency are the two variables of main concern in terms of industry standard stability, as shown in Figures 7 and 8, which is why they were selected for detailed analysis. Although the phase angle is the third critical indicator of grid stability, in addition to voltage and frequency, it was not focused on in the scope of this project.

Comparing the voltage and frequency graphs to the industry standards mainly involved visually assessing if the frequency and voltage stayed within the "No Trip Zone". If the graphs showed values within these boundaries, then it was safe to conclude that the electricity being supplied to the school was stable. If any frequency or voltage values were close to the boundaries of the "No Trip Zone" after visual assessment, the graphs were analyzed in the software right

after the simulation was run, so that the cursor could trace over exact values. Close to the boundaries meant that the resolution of the y-axis created too much uncertainty in the value of the voltage or frequency that it could not be concluded with absolute certainty that the voltage or frequency fell within its respective "No Trip Zone".

5 Results

For each type of inverter, the full ten second simulation results are given for the system. These results are zoomed out and only show general trends, so no strong conclusions can be made from them. Therefore, simulation results for the frequency and voltage of the system are zoomed in at 3 seconds, 5 seconds, and 7 seconds, to see how the system reacted to the different transients that happen at these timestamps. The beginning of the simulation will show instability as the system starts up, these few tenths of a second will not be analyzed since this model is mainly concerned with how the different inverter react to transients when the solar farm and grid are already up and running.

5.1 Full 10 Second Simulation Results of the System

For all results of the system, the voltage, active power, and reactive power are measured at each bus. For the voltage, active, reactive power results, bus 1 results are in blue, bus 2 in green, and bus 3 in maroon. The apparent power (MVA) is measured at bus 1, and the load frequency (Hz) is measured at bus 2. The location of each bus is shown in Figure 6.

The results from the full system help to point out differences between the different inverter types. While the analysis of these simulation results is mainly focused on the voltage and frequency results near the load, these full system results show general trends of how apparent, active, and reactive power, all react to transients. These preliminary results about power could be analyzed in the future to better understand system stability.

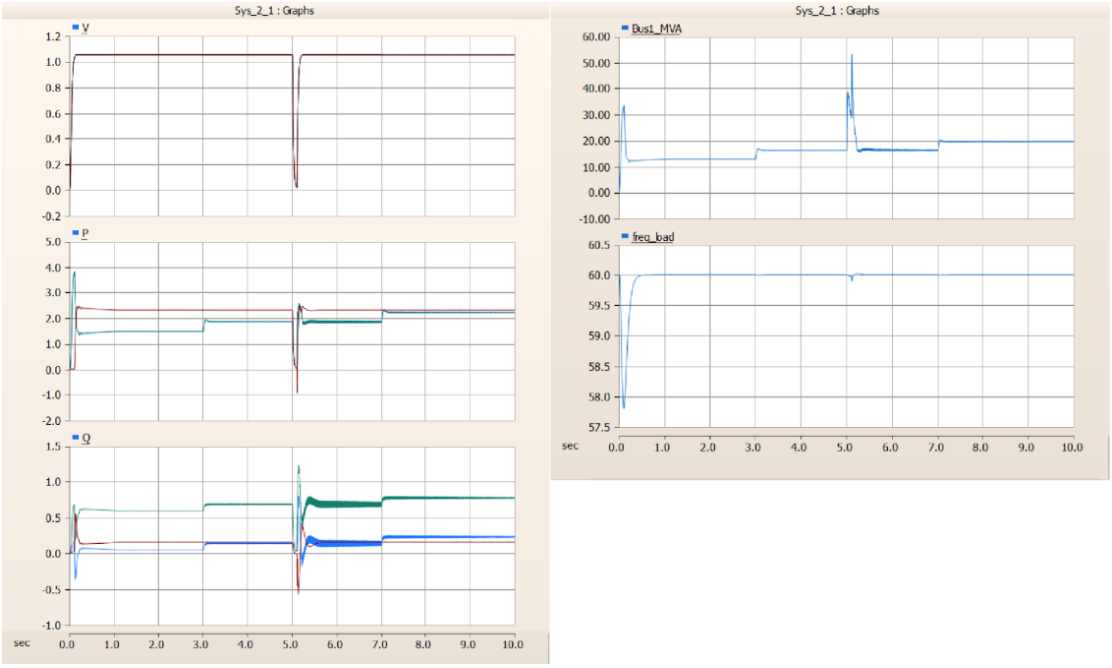

Figure 11: Full simulation results of the system when the inverter is in GFL mode with three transients: a 10% load increase at 3 seconds and 7 seconds, and a three-phase ground to fault at 5 seconds. For the voltage, active, reactive power results, bus 1 results are in blue, bus 2 in green, and bus 3 in maroon. The apparent power (MVA) is measured at bus 1, and the load frequency (Hz) is measured at bus 2. The location of each bus is shown in Figure 6. Starting from the top graph, the voltage amplitude graph (in per-unit, PU) shows stability near the 1.05 PU reference that is set at the voltage source and at the solar farm, and the dip coincides with the transient at 5 seconds. Because of this large dip, the y-axis has low resolution (0.2pu) the three bus measurements overlap and only display one line. The active power graph, P (MW), shows bus 3 results that are coming from the solar farm power generation, and the bus 1 and bus 2 lines are overlapped and show the active power generated from the voltage source. The bus 1 and bus 2 active power increases with the load increase at 3 and 7 seconds and, along with bus 3, show a dip and spike with the fault at 5 seconds. The bus 3 line dips with the fault at 5 seconds. The reactive power graph, Q (MVAR), shows separate reactive power values for each bus. All three of which show instability during the fault at 5 seconds, and the bus 1 and bus 2 reactive power increase during the increase in load at 3 seconds and 7 seconds. The apparent power (MVA), only measured at bus 1, increases when the load increases at 3 seconds and 7 seconds, and shows a large spike during the fault at 5 seconds, but it recovers shortly after the fault. Finally, the frequency, at bus 2, holds around the set 60 Hz, showing a small instability during the fault at 5 seconds. At this scale GFM inverter results for voltage and frequency are the same.

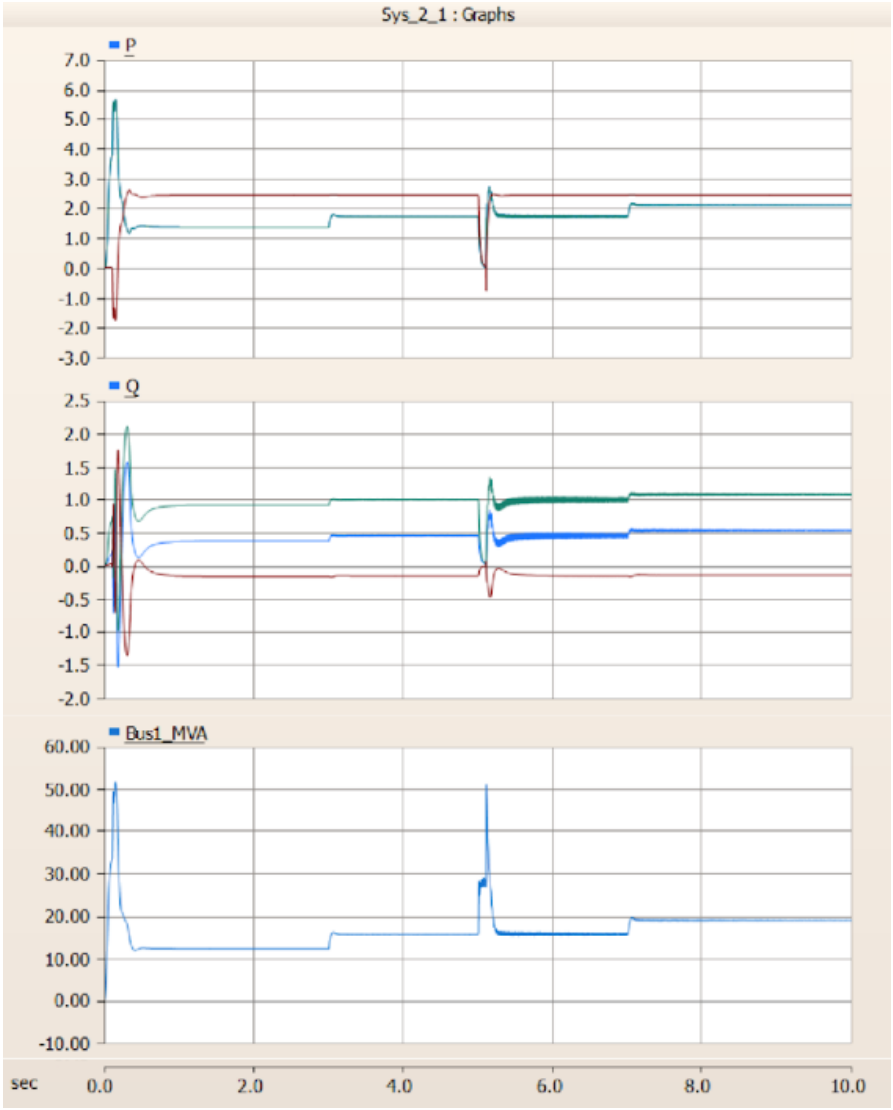

Figure 12: Active power, reactive power, and apparent power full simulation results from the system when the inverter is in GFM droop control mode. V and freq the same (delete graphs). Bus 1 (blue) and bus 2 (green) start at lower active power value than GFL results, but exhibit the same instability during transients. The apparent power has a similar, but different shaped peak at the 5 second transient than GFL results. The reactive power graph shows the reactive power from bus 3 (red) at a negative value. All buses show instability in reactive power during the fault at 5 seconds and bus 1 and 2 show an increase in reactive power at 3 seconds and 7 seconds when the load increases. GFM VSM has the same active power, reactive power, and apparent power results. GFM VOC has the same apparent power results.

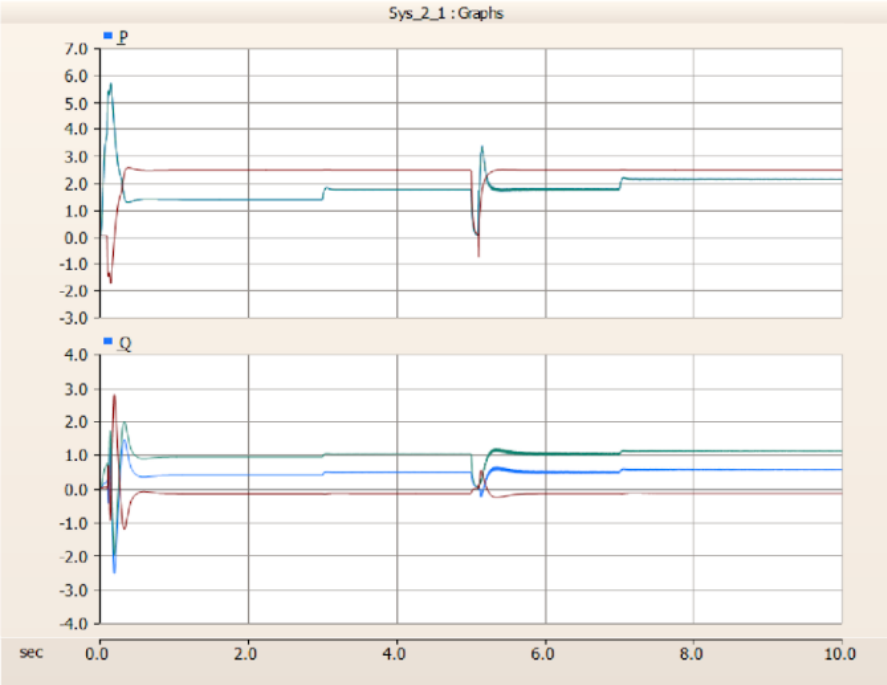

Figure 13: Active and reactive power full simulation results from the system when the inverter is in GFM VOC mode. The active power spike at bus 1 (blue) and 2 (green) at 5 seconds due to the fault is higher than other GFM results. Compared to the other GFM inverter results, the reactive power at bus 1 and 2 do not spike as much at 5 second transient, and at bus 3 (red) the reactive power does not dip as much.

From these results a handful of differences can be noted between the four inverter types.

The voltage level graphs do not offer any noticeable differences. At this scale and level of detail the graphs are virtually the same across all inverter types, and react similarly to the transients.

Across all the inverters, the active power at bus 3 is stable with a dip when there is a fault at 5 seconds. The active power at bus 3 is lower for GFL results in Figure 11, than GFM results in Figure 12. For the GFL inverter the active power at bus 1 and 2 starts close to 1.5MW and increases by about 0.4MW when the load increases at 3 seconds and 7 seconds as shown in Figure 11. The increase in bus 1 and 2 active power happens across all inverter types, although the bus 1 and bus 2 active power start at a slightly lower active power in GFM inverter results in Figure 12 than the GFL inverter results in Figure 11. During the fault at 5 seconds all inverter types show the same response in active power, except for VOC, which has a higher active power spike at bus 1 and 2 as shown in Figure 13. Since each inverter uses slightly different methods to regulate its frequency, it is not surprising to see different inverters injecting different levels of active power to control its frequency during the different transients.

The reactive power graphs show the most noticeable differences across the four inverter type results. Note that the y-axis scale is different for each inverter type across the reactive power results. First, to note a similarity, all four inverter results show an increase in reactive power at bus 1 and 2 when the load increases at 3 and 7 seconds. The GFM inverter results show higher reactive power levels at bus 1 and 2 than the GFL inverter results. The bus 2 reactive power stays close to 1 MVAR and bus 1 close to 0.5 MVAR when the solar farm is using any GFM inverter (see Figures 12 and 13), while if the solar farm is in GFL mode the bus 2 reactive power is lower, starting just above 0.5 MVAR and ending close to 0.8 MVAR, and the bus 1 reactive power is also lower, always staying below 0.4 MVAR, except for during the fault at 5 seconds, as shown in Figure 11. While GFM inverter results have higher reactive power levels at bus 1 and 2, they also have lower, and negative, reactive power at bus 3 than the GFL inverter results. The GFL inverter results show the bus 3 reactive power is steady around 0.2 MVAR, except

for during the fault at 5 seconds, see Figure 11. While for the GFM inverter results, the bus 3 reactive power falls just below 0, around -0.15 MVAR, as shown in Figures 12 and 13. During the fault at 5 seconds, all reactive power results show instability. The GFL inverter results show more instability during this fault as the reactive power has a larger dip and spike at all three buses, see Figure 11, compared to the GFM inverter results, see Figures 12 and 13. The VOC results show the most stability during this fault at 5 seconds, with very small spikes at bus 1 and 2, and a very small dip at bus 3, as shown in Figure 13. Each inverter uses different control methods, so it makes sense to see some variability in the amount of reactive power each inverters would inject to control the voltage. Since GFL inverter control is inherently different than GFM control, while each GFM control method has similar goals, it is reasonable that GFM inverter results overlap.

Now looking at the results of the apparent power measured at bus 1, all inverter types show very similar results. All results show an increase in apparent power when the load increases at 3 seconds and 7 seconds, and all show a spike to about 50 MVA during the fault at 5 seconds. The only notable difference is the GFL inverter graph shows a differently shaped spike at 5 seconds, see Figure 11, compared to the spikes at 5 seconds from the GFM results, shown in Figures 12 and 13.

The frequency results from bus 2 are the same across all inverter types at the scale and level of detail given from these full system results.

5.2 Voltage and Frequency Results During the Three Transients

5.2.1 Transient at 3 Seconds

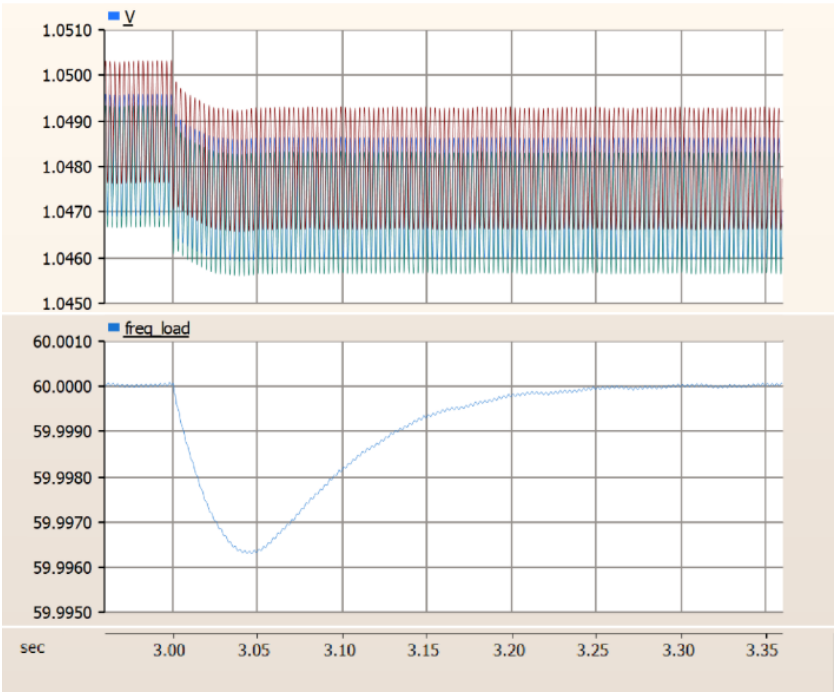

Figure 14: GFL inverter simulation results from the system of the voltage and frequency near the load during the 10% increase in load at 3 seconds. The voltage amplitude (PU) results display the three voltage levels from each bus. Due to the increase in load at 3 seconds, the voltage drops from a high point of 1.0503 PU to 1.0493 PU. The voltage range between the three buses is about 0.0036 PU. The frequency (freq load) results are measured at bus 2 in hertz. After the transient at 3 seconds the frequency drops from 60 Hz to 59.9964 Hz before recovering back to 60 Hz 0.3 seconds after the load increase. Notice how the frequency lines exhibit slight oscillation.

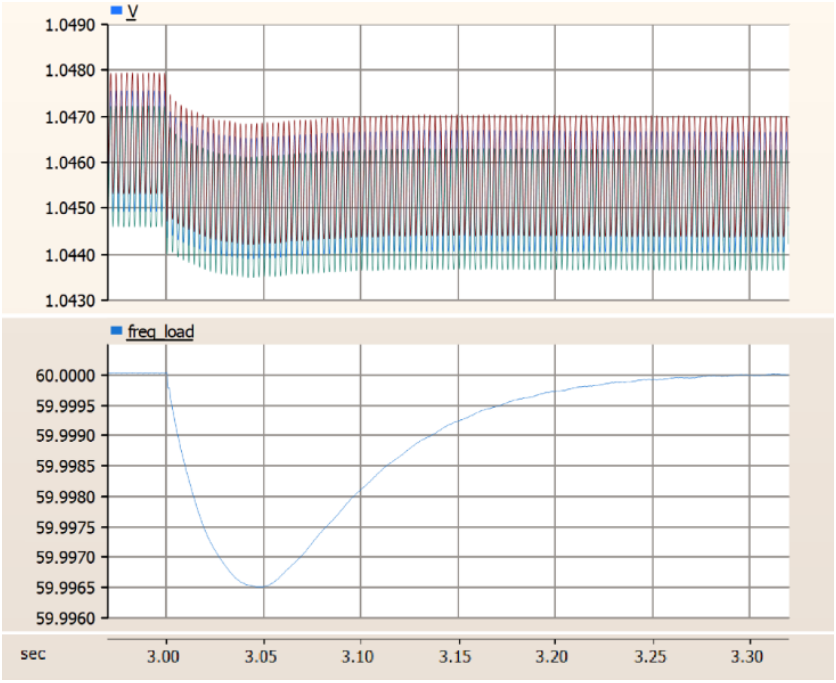

Figure 15: GFM droop control simulation results from the system of the voltage and frequency near the load during the 10% increase in load at 3 seconds. The voltage amplitude (PU) for each bus is graphed. The resting voltage levels before and after the transient are lower than the GFL results and the voltage range (about 0.0033 PU) is smaller than the GFL results. The frequency (Hz) is measured at bus 2. The frequency drops to 59.9965 Hz, 0.0001 Hz less of a drop than the GFL results. The recovery time of the frequency back to 60 Hz is the same as the GFL results, except GFM frequency exhibits no oscillation. These results for GFM droop are the same for both GFM VSM and GFM VOC.

5.2.2 Transient at 7 Seconds

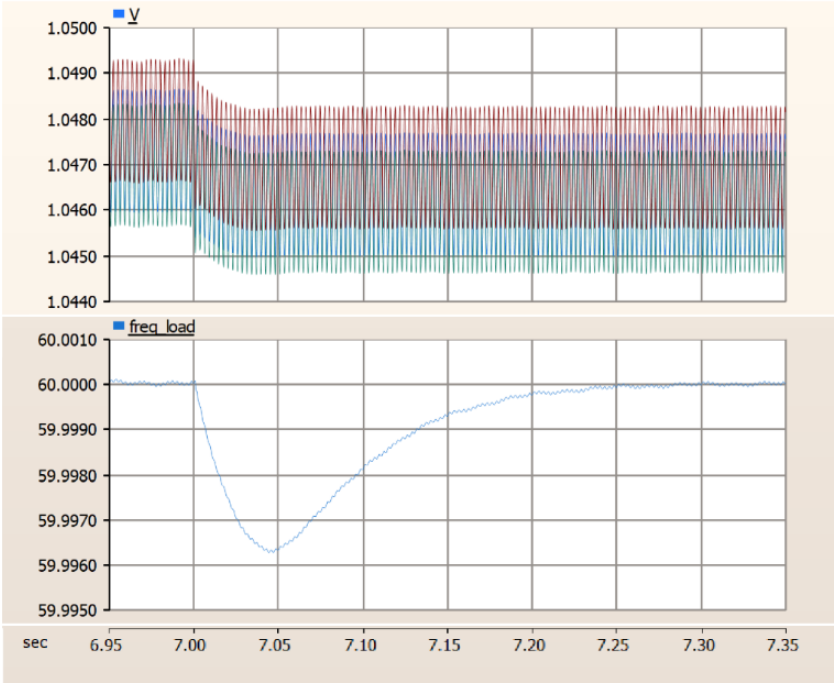

Figure 16: GFL inverter simulation results from the system of the voltage and frequency near the load during the 10% increase in load at 7 seconds. The voltage amplitude (PU) for each bus is graphed. Due to the increase in load at 7 seconds, the voltage drops from a high point of 1.0493 PU to 1.0483 PU. The voltage range between the three buses is about 0.0036 PU. The frequency (Hz) is measured at bus 2. After the transient at 3 seconds the frequency drops from 60 Hz to 59.9964 Hz before recovering back to 60 Hz 0.3 seconds after the load increase. Notice how the frequency lines exhibits slight oscillation.

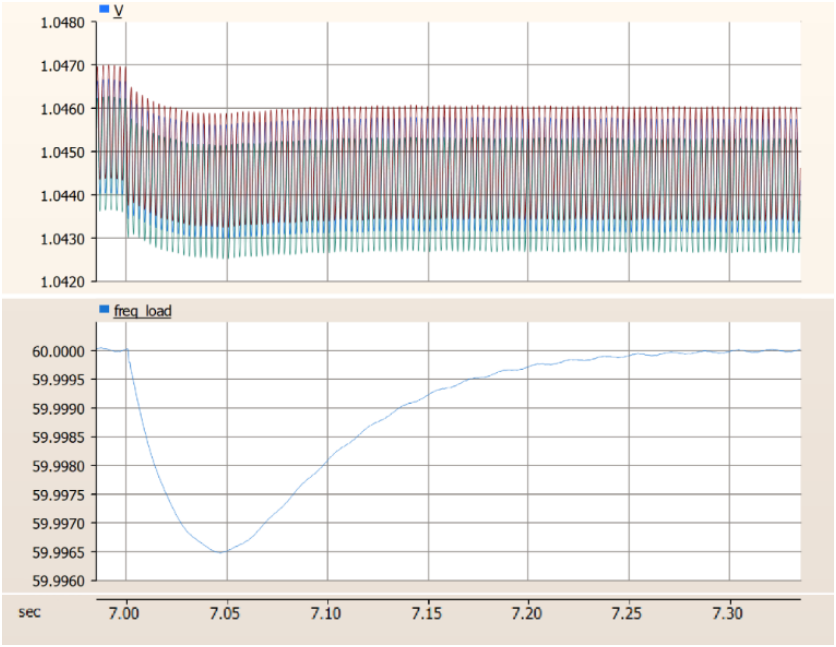

Figure 17: GFM droop control inverter simulation results from the system of the voltage and frequency near the load during the 10% increase in load at 7 seconds. The voltage amplitude (PU) for each bus is graphed. These resting voltage levels before and after the transient are lower than the GFL results and the voltage range (about 0.0033 PU) is smaller than the GFL results. The frequency (Hz) is measured at bus 2. The frequency drops to 59.9965 Hz, 0.0001 Hz less of a drop than the GFL results. The recovery time of the frequency back to 60 Hz is the same as the GFL results. GFM frequency results exhibit no oscillation. These results for GFM droop are the same for both GFM VSM and GFM VOC.

Examining the voltage results during these 10% increases in load shows that the voltage only drops 0.001 PU for all inverter types at 3 seconds and 7 seconds as shown in Figures 14, 15, 16, and 17. The GFL and GFM inverter results differ in the voltage level they start at. The GFL inverter results, before the transient at 3 seconds, has its highest voltage, peak just above 1.05 PU, as shown in Figure 14, while the GFM inverter results show the voltage peaks closer to 1.048 PU as shown in Figures 15. It is expected to see a small difference in voltage since GFM inverters use different control methods for voltage than GFL inverters.

The frequency also changes during the transients at 3 seconds and 7 seconds. When the load increases the GFL frequency results drop from 60 Hz to a low point of 59.9964 Hz before fully recovering back to 60 Hz after 0.3 seconds as shown in Figures 14 and 16. The GFM results show a slightly smaller drop in frequency, dropping to 59.9965 Hz, as shown in Figure 15 and 17. Since GFL and GFM inverters use different control methods to calculate frequency, it is expected that these results would slightly differ.

The frequency recovers at the same rate for all four inverter types, but the plotted frequency line for the GFL results shows a small level of oscillation, see Figure 14, when compared to the frequency in the GFM results shown in Figure 15.

5.2.3 Solid Three-Phase to Ground Fault for 0.1s at 5 Seconds

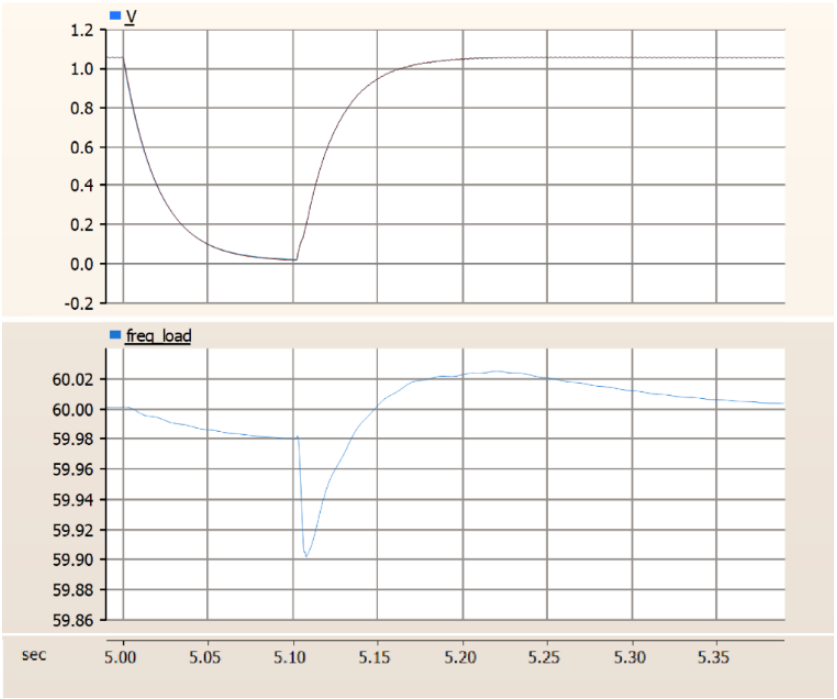

Figure 18: GFL inverter simulation results from the system of the voltage and frequency near the load during the solid three-phase to ground fault for 0.1s at 5 seconds. At the current y-axis scale (0.1 PU resolution) the three bus measurements overlap and only display one line. The frequency results (freq load) are from measurements at bus 2 and reported in hertz.

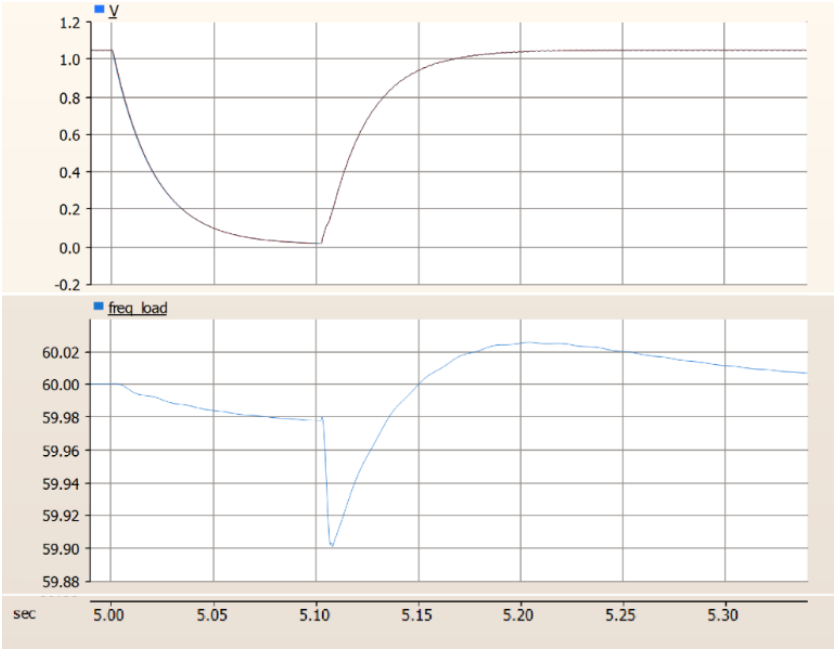

Figure 19: GFM droop control simulation results from the system of the voltage and frequency near the load during the solid three-phase to ground fault for 0.1s at 5 seconds. The voltage (PU) measurements at each bus (overlapped). The frequency (Hz) results from measurements at bus 2. GFM VSM and GFM VOC have the same results.

The transient at 5 seconds, the solid three-phase to ground fault for 0.1 seconds, shows similar voltage recovery for all four types of inverters. Within 0.15 seconds from the fault, the voltage recovers back above 0.9 PU, and after 0.2 seconds the voltage stabilizes near 1.05 PU, where it was before the transient. This recovery trend is shown in Figures 18 and 19.

During the solid three-phase to ground fault the frequency slowly decreased for 0.1 seconds, then after the fault is cleared the frequency dips to a low point of 59.90 Hz before recovering and peaking just above 60.02 Hz before recovering back to 60 Hz approximately 0.4 seconds later as shown in Figures 18 and 19.

6 Discussion

6.1 Voltage Recovery

Voltage recovery in both the GFL and GFM inverter results showed sufficient voltage recovery during all three transients according to industry standards shown in Figure 7.

6.1.1 Voltage Recovery During an Increase in Load

During the 10% increase in load at 3 seconds and 7 seconds the voltage only drops 0.001 PU as shown in Figures 14, 15, 16, and 17. This small drop in voltage occurs because the increase in load is drawing more reactive power from the grid. This causes that the solar farm and grid to respond by supplying more reactive power, which means more reactive current will flow through the network reactance, producing a voltage drop. Unlike frequency, voltage has no inertial behavior and therefore settles at a new steady-state value rather than recovering automatically. Although GFL inverters do not establish voltage through the Q–V relationship, they still measure and respond to changes in grid conditions. Since power is being supplied from the grid, in addition to the solar farm with GFL inverters, the grid will respond to the change in reactive power by adjusting the system voltage and the GFL inverters will follow this response. Therefore, small voltage deviations caused by load increases appear in both GFL and

GFM results, leading to similar behavior in a stiff network. This voltage change is an extremely small and is well within the "No Trip Zone" standards for voltage shown in Figure 7.

6.1.2 Voltage Recovery During a Solid Three-Phase to Ground Fault

Please refer to Figures 18 and 19 for results of the voltage during the fault. Since all four inverter types have the same voltage results during this transient, any reference made to voltage level during this section of the discussion can be seen in any of the four Figures.

The transient at 5 seconds, the solid three-phase to ground fault for 0.1 seconds, shows similar voltage recovery for all four types of inverters. During a fault, current travels through a low-impedance return path, which causes large currents and a collapse in voltage. This is why the voltage drops almost to 0 PU during the fault. Shortly after the fault is cleared, after 0.1 seconds in the simulation, the voltage recovers within 0.15 seconds. This quick recovery is because normal network impedance is restored and GFM sources, either the grid or GFM inverters, quickly re-establish the voltage. Although there are slightly different voltage levels between GFL and GFM inverter results, as discussed in the previous section (6.1.1), the resolution of the voltage level results during the fault is 0.2 PU because the voltage dips nearly to zero. This level of voltage resolution coupled with a stiff grid that can lead the voltage recovery for the GFL inverters is why the GFL and GFM inverter results are the same for this fault.

The "No Trip Zone" standards allow for the voltage to fall below 0.45 PU for 0.15 seconds and below 0.65 PU for 0.3 seconds as shown in Figure 7. While the voltage does fall below 0.45 PU, it is below this threshold for 0.1 seconds before rapidly recovering back above 1.0 PU. With the whole voltage dip happening within 0.2 seconds, it stays within the "No Trip Zone" since it is not below 0.65 PU for longer than 0.3 seconds.

6.1.3 Difference in Voltage Recovery for GFL Inverter Results vs. GFM Inverter Results

The only difference between inverter types when examining voltage level during these transients is the stable voltage level during the 3 second and 7 second increases in load. The GFL inverter results show that before the transient at 3 seconds the highest voltage, from bus 3 in red, rests just above 1.05 PU as shown in Figure 14 while the GFM inverter results show a resting high voltage, again from bus 3 in red, closer to 1.048 PU as shown in Figure 15. These slight differences in steady-state voltage levels between the GFL and GFM inverter results are a consequence of their control strategies. GFM inverters supply reactive current to regulate voltage, resulting in a small voltage drop across the physical network impedance. Physical network impedance refers to the inherent impedance of the LCL filter, transformer, and lines through which inverter current flows. GFL inverters rely on the grid to supply most of the reactive power, allowing bus voltages to remain closer to the grid-regulated setpoint. The resulting voltage difference is therefore a consequence of GFM inverters' reactive power sharing rather than inferior voltage regulation.

Although GFM inverters actively regulate voltage, the drop in voltage during the increase in load is the same for the GFL and GFM inverter results. This can most likely be attributed to the stiff-grid configuration considered in this study. Differences between control strategies in GFL vs. GFM inverters primarily affect the steady-state operating point rather than the short-term voltage drop.

The GFL inverter demonstrates it is capable of properly stabilizing voltage for Hamilton College as the simulation results are consistent with industry standards.

6.2 Frequency Recovery

The frequency recovery for all four different types of inverters complied with the industry frequency standards in Figure 8.

6.2.1 Frequency Recovery During an Increase in Load

During the increase in load at 3 seconds and 7 seconds all inverters had a frequency drop from 60 Hz to a low point of 59.9965 Hz before fully recovering back to 60 Hz after 0.3 seconds as shown in Figures 14, 16, 15, and 17. The results showing a drop in frequency when the load increases follows the established relationship between active power and frequency. The load increase is drawing more active power from the solar farm and grid, which cannot instantaneous produce more power, so the frequency will drop before it recovers as the solar farm and grid work to meet the increased demand in active power. Similar to the explanation about why the GFL inverter results still showed a dip in voltage when reactive power increased, the GFL inverter results show a frequency droop because it is following the grid. The GFL inverter does not establish its frequency through the P–ω relationship, but since the grid is also supplying power to the system, the GFL inverter will follow the grid's drop and recovery in frequency.

This frequency recovery falls well within the limits of the "No trip zone" for Eastern Interconnection. The frequency would have had to fall below 58 Hz or well above 61 Hz in a 0.3 second time frame to land outside the "No Trip Zone" as shown in Figure 8.

6.2.2 Frequency Recovery During a Solid Three-Phase to Ground Fault

Please refer to Figures 18 and 19 for results of the frequency during the fault. Since all four inverter types had the same frequency results during this transient, any reference made to frequency level during this section of the discussion can be seen in any of the four Figures.

During the solid three-phase to ground fault for 0.1 seconds at 5 seconds, the frequency slowly decreased during the fault, then dipped to a low point of 59.90 Hz before recovering back to 60 Hz approximately 0.4 seconds later. Established earlier, during the 0.1 s three-phase fault, voltage collapses. This means that active power delivery from source to load is severely reduced, but the demand for active power from the load has not changed. This imbalance causes the decrease in frequency from 5 seconds to 5.1 seconds. After the fault is cleared, at 5.1 seconds, the results from all four inverters show a sudden dip in frequency. This is because immediately after the fault is cleared, voltage is restored almost instantly, which allows the load to draw active power again. Generation cannot output active power at the rate the load draws the power, resulting in a deeper frequency dip. As generation increases active power production, the frequency recovers with a damped, exponential response. Then the frequency briefly overshoots the nominal 60 Hz, rising just above 60.02 Hz before returning to 60 Hz. This overshoot is expected because after the fault is cleared more active power than required is injected to control the frequency. This frequency control causes the system to overshoot 60 Hz before it reduces the active power and frequency settles back towards 60 Hz. The GFL inverter recovers in the same way as GFM inverter because it is synchronized to a strong grid that establishes frequency, and the grid is stiff enough to dictate the post-fault recovery.

This frequency recovery is well within the "No Trip Zone". Values of 60.02 Hz and 59.90 Hz are close enough to 60 Hz that they fall within the "No Trip Zone" regardless of the length of time as shown in Figure 8.

6.2.3 Difference in Frequency Recovery for GFL Inverter Results vs. GFM Inverter Results

A small, but noticeable, difference in the frequency support between the GFL and GFM inverters is revealed in the stability of the frequency line during the increase in load at 3 seconds and 7 seconds. For example, when comparing GFL results from Figure 14 to the GFM results in Figures 15 the frequency line in the GFL results oscillates slightly. This demonstrates how GFM inverters are more stable than GFL, but in this case, with the amount of stability provided from the voltage source, that very small increase in stability is not significant.

The GFL inverter, with the given support from the grid, demonstrates it is capable of properly stabilizing frequency for Hamilton College and provides nearly equivalent frequency control to GFM inverters in this modeled system. Using GFL inverters would be the best option for

Hamilton College's solar farm as it provides nearly equivalent frequency control to GFM inverters and is easier to maintain and cheaper to procure.

6.3 Assumptions/Limitations and Future Steps

Although this experiment offers a conclusion, there were several important assumptions and limitations that must be addressed:

- **Model Design Assumptions:** There were serval generalized assumptions made when creating the Hamilton College PSCAD model. The main assumption is that the stiffness of the simulated grid models the stiffness of the actual utility grid Hamilton College relies on. If the actual utility grid is more or less stiff than in the simulation, then conclusions about GFL inverters being sufficient could be inaccurate. Also, the current design generalized the transformer, which steps the voltage down from the utility grid to Hamilton, from two transformers in parallel to a single transformer. Additionally, the expected power factor of the load should be verified. Finally, this simulation uses a smaller solar farm, compared to the initial larger plan. The solar farm scale will likely affect both the capacity and operational characteristics of the system, which should be modeled carefully for accurate results.
- **Quantitative Assessment Limitations:** While the analysis has focused on qualitative assessments and visualizations (graphs of the three transient scenarios), there is a need to conduct more detailed quantitative evaluations. This would include collecting exact data of frequency or voltage deviations, and pushing the analysis beyond just determining if these variations comply with industry standards.
- **Active Power, Reactive Power, and Phase Angle Analysis:** Another limitation of this experiment was it did not fully analyze power or phase angle results. Further investigation into the active and reactive power dynamics during transients can add another layer of understanding grid stability. Reactive power control is particularly important for voltage regulation, and understanding how GFL and GFM inverters manage this under fault conditions will clarify the overall system stability. For instance, while both VSM and droop control strategies exhibit similar performance in reactive power regulation, the VOC strategy appears to provide potentially stronger reactive power control. This could have implications for voltage stability during grid faults although these were not shown in this experiment's results given how stiff the system was. Furthermore, the observed spike in active power during fault conditions, especially the higher spike in VOC results, needs deeper analysis to determine if this behavior is due to the inverter's control settings, the nature of the fault, or both. Also, despite the importance of phase angle in grid stability, this variable was not reported or analyzed in this experiment. Although given the promising results of frequency and voltage, it is likely phase angle would follow suit.

There also are a variety of future experiments and steps that could be evaluated:

- **Grid-Disconnected Operation (Off-Grid):** A key consideration is the potential transition of the college to an independent grid system, powered solely by the solar farm. This shift will directly impact the inverter choice, as the inverters must handle variations in frequency and voltage in an isolated environment without grid support. This experiment would evaluate how different inverter types will perform when disconnected from the grid, particularly in terms of GFM inverters' ability to maintain stability and balance without grid voltage references. Since GFL inverters cannot function without a grid voltage reference, this would mainly involve comparing different GFM inverters.
- **Fault Impact and 'No Trip Zone' for Frequency and Voltage:** Another aspect to explore is what kind of load changes or faults could cause the system to fall outside the 'No Trip Zone' for frequency or voltage. Specifically, understanding the boundary conditions for each inverter type and how they interact with the grid or isolated system during disturbances could be interesting.

7 Conclusion

This thesis evaluated the stability provided by different inverter types for a potential Hamilton College solar farm that would operate while the college remains interconnected with the utility grid. This study concludes that grid-following inverters provide sufficient stability while offering the most practical and cost-effective solution. As inverter-based resources, such as renewable energy, continue to replace synchronous generators, selecting an inverter that maintains voltage and frequency stability is increasingly important. To address this question, a model of the Hamilton College electrical system was developed in PSCAD and used to compare grid-following (GFL) inverters with three grid-forming (GFM) control strategies: droop control, virtual synchronous machine (VSM), and virtual oscillator controllers (VOC).

Simulation results demonstrated that, under three different transients, including two 10% increases in load and a solid three-phase-to-ground fault, voltage and frequency remained well within established industry "no-trip" zones for all four inverter types. The presence of a stiff utility grid dominated overall system behavior, limiting deviations in both voltage and frequency and ensuring rapid recovery following disturbances. While GFM inverters exhibited smoother frequency responses and slightly different voltage support during load increases, these differences did not point to meaningful advantages for Hamilton's power system stability in this grid-connected configuration. Given that GFL inverters are less expensive, simpler to implement, and require less maintenance than GFM alternatives, the results indicate that a grid-following inverter is the most appropriate choice for a Hamilton College solar farm under the modeled conditions.

Future work could explore scenarios in which the campus operates in a weak-grid or islanded configuration, where the benefits of grid-forming inverters may become more significant. Additional studies could also examine larger or longer-duration transients. Regardless, for the present system: a solar installation connected to an already grid-connected campus, this thesis concludes that GFL inverters provide sufficient stability while offering the most practical and cost-effective solution.

References

[1] Yashen Lin, Joseph Eto, Brian Johnson, Jack Flicker, Robert Lasseter, Hugo Villegas Pico, Gab-Su Seo, Brian Pierre, and Abraham Ellis. Research roadmap on grid-forming inverters. Technical Report NREL/TP-5D00-73476, National Renewable Energy Laboratory, 2020.

[2] Deepak Ramasubramanian. Epri grid forming inverter models. Technical report, Electric Power Research Institute (EPRI), Palo Alto, CA, November 2022. Revision 1.

[3] Paul Horowitz and Winfield Hill. *The Art of Electronics*. Cambridge University Press, Cambridge, UK, 3 edition, 2015.

[4] Maya Posch. Power grid stability: From generators to reactive power. `https://hackaday.com/2025/07/22/power-grid-stability-from-generators-to-reactive-power/`, July 22 2025. Accessed: 2025-9-20.

[5] Eduard Muljadi, Mohit Singh, and Vahan Gevorgian. User guide for pv dynamic model simulation written on pscad platform. Technical Report NREL/TP-5D00-62053, National Renewable Energy Laboratory, Golden, CO, 2015.

[6] Deepak Ramasubramanian and Evangelos Farantatos. Generic positive sequence domain model of grid forming inverter based resource. Technical Report 3002021403, Electric Power Research Institute (EPRI), Palo Alto, CA, 2021. Technical Update, December 2021.

[7] Brian Johnson, T. G. Roberts, Olaoluwapo Ajala, Alejandro Dominguez-Garcia, Sairaj Dhople, Deepak Ramasubramanian, Aidan Tuohy, Deepak Divan, and Benjamin Kroposki. A generic primary-control model for grid-forming inverters: Towards interoperable operation & control. *Proceedings of the Hawaii International Conference on System Sciences*, pages 1–10, 2022.

[8] Pscad official website. https://www.pscad.com. Accessed: 2025-08-30.

[9] NERC. Prc-024-3 — frequency and voltage protection settings for generating resources. https://www.nerc.com/globalassets/standards/reliability-standards/prc/prc-024-3.pdf, 2020. Accessed: 2025-12-03.

[10] Cps 250 kw 600 v datasheet. Technical report, Chint Power Systems, July 2025. PDF datasheet for inverter used in land lease proposal.

[11] PSCAD User Guide. Photovoltaic example written for pscad v4.6, September 2018. Revision 1.

A Appendix

SOLARLIBERTY®

Technical Aspects of the Proposal
Ground Mounted Single-Axis Tracker

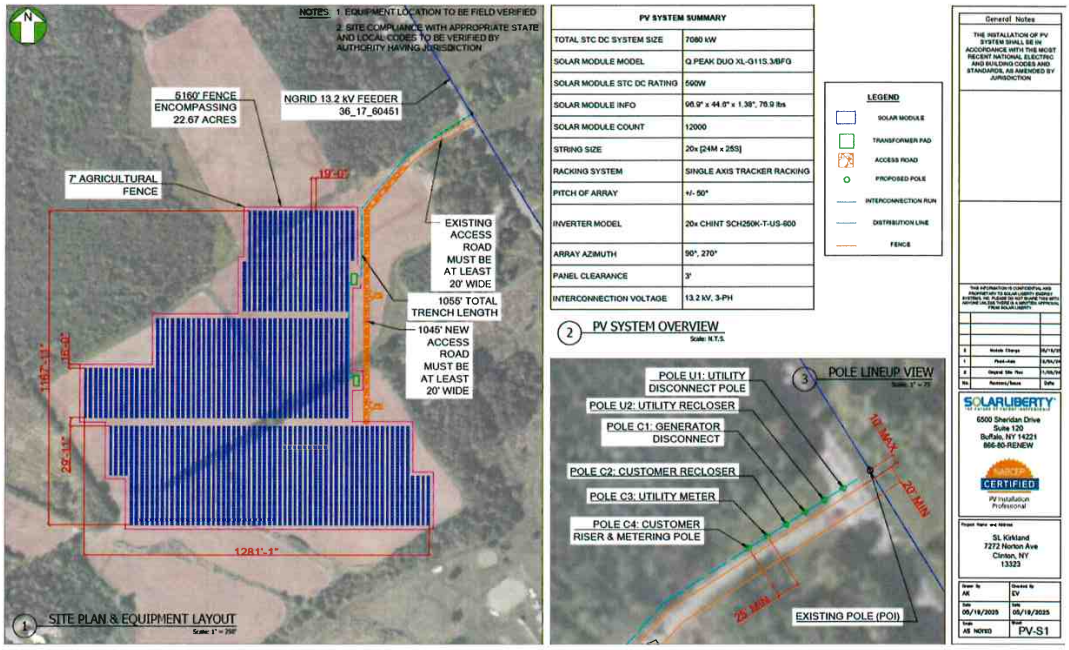

Full size document included in supporting documents

System Components & Design

- **Inverters**:
  - Model: CHINT SCH250K-T-US-600
  - Quantity: 20 units
  - Each inverter rated at 250 kW (AC)
  - Combined Inverter Output: 5,000 kW (AC)
- **Interconnection & Electrical Design**:
  - Interconnection Voltage: 13.2 kV, 3-phase
  - POI: Existing utility pole with interconnection via National Grid's 13.2 kV Feeder #36_17_60451
  - Total trench length for interconnection: 1,055 ft
  - Utility Poles: Includes utility disconnect, reclosers, metering poles, and customer disconnect infrastructure for code-compliant and utility-accepted integration

13

Figure 20: Details for Hamilton College's land lease solar farm. Note the rated active power output as well as the specific inverter model, which was further researched to find voltage information given in reference [10]. Details shared by Daniel Rodriguez Rosario (derodrig@hamilton.edu)

Extra GFM (identical to GFM Droop control) results:

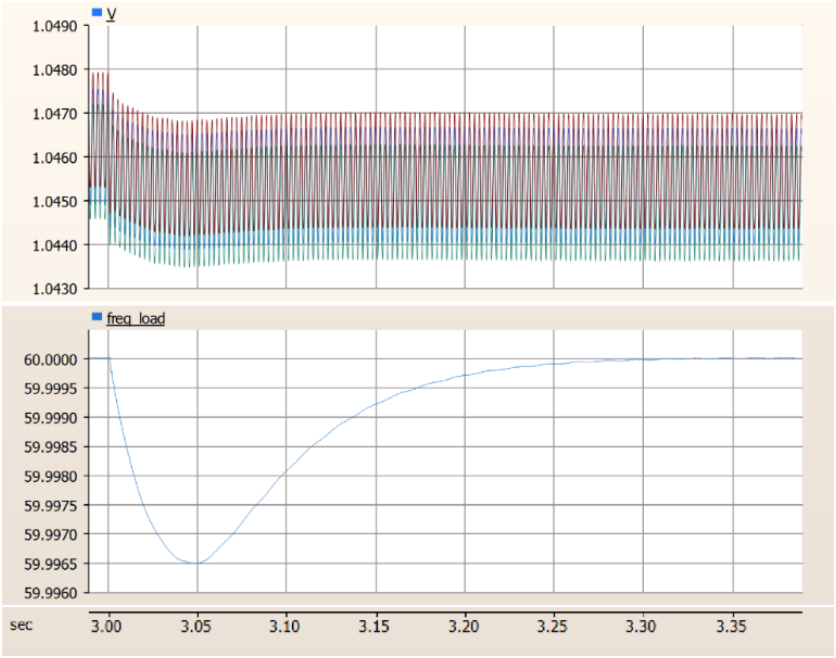

Figure 21: GFM VSM control simulation results from the system of the voltage and frequency near the load during the 10% increase in load at 3 seconds. The voltage amplitude (PU) for each bus is graphed. The frequency (Hz) measured at bus 2.

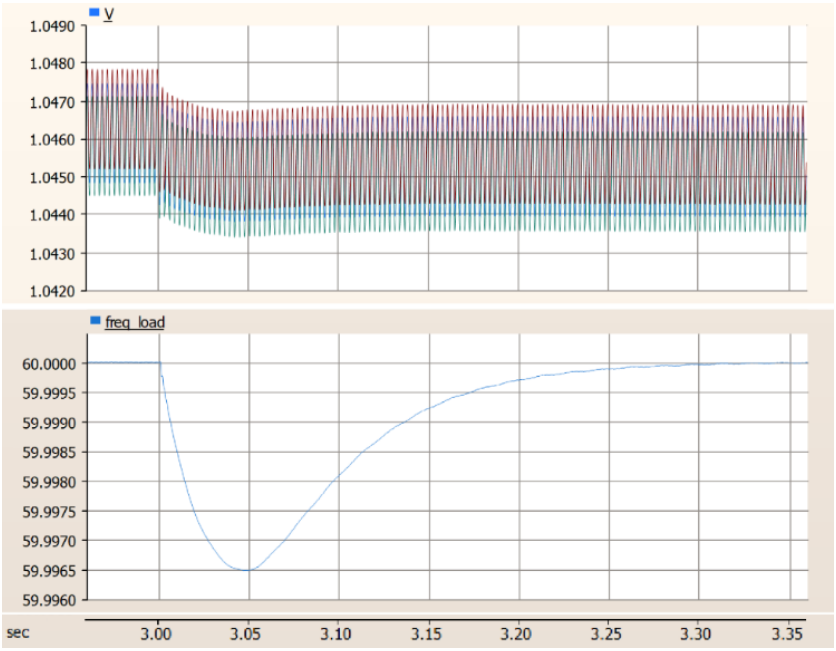

Figure 22: GFM VOC simulation results from the system of the voltage and frequency near the load during the 10% increase in load at 3 seconds. The voltage amplitude (PU) for each bus is graphed. The frequency (Hz) measured at bus 2.

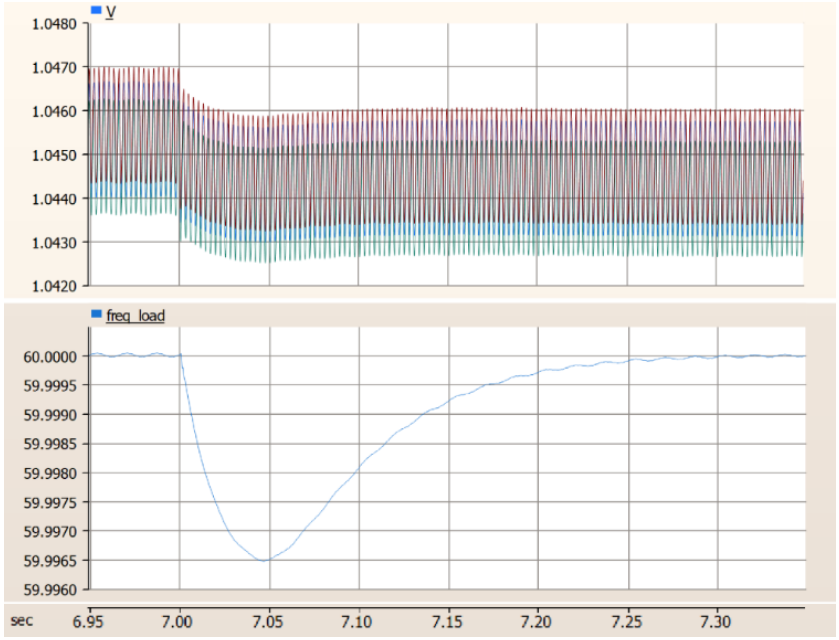

Figure 23: GFM VSM control inverter simulation results from the system of the voltage and frequency near the load during the 10% increase in load at 7 seconds. The voltage amplitude (PU) for each bus is graphed. The frequency (Hz) measured at bus 2.

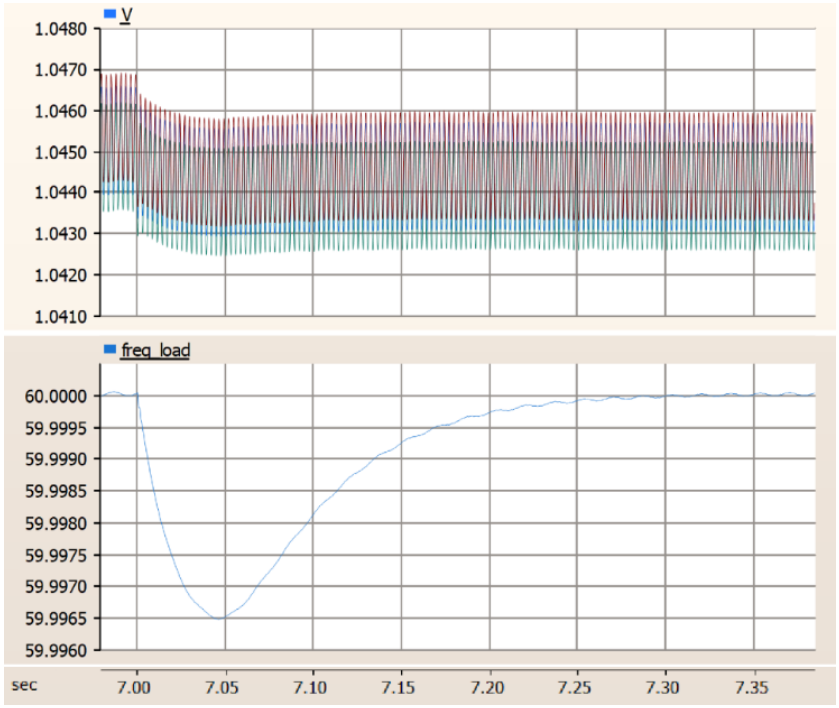

Figure 24: GFM VOC inverter simulation results from the system of the voltage and frequency near the load during the 10% increase in load at 7 seconds. The voltage amplitude (PU) for each bus is graphed. The frequency (Hz) measured at bus 2.

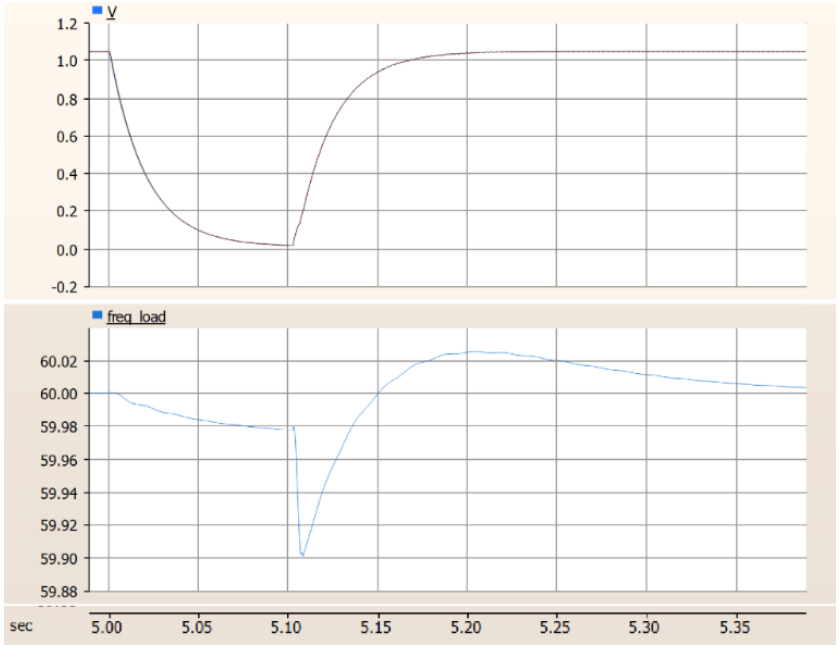

Figure 25: GFM VSM control simulation results from the system of the voltage and frequency near the load during the solid three-phase to ground fault for 0.1s at 5 seconds. The voltage (PU) measurements at each bus (overlapped). The frequency (Hz) results from measurements at bus 2.

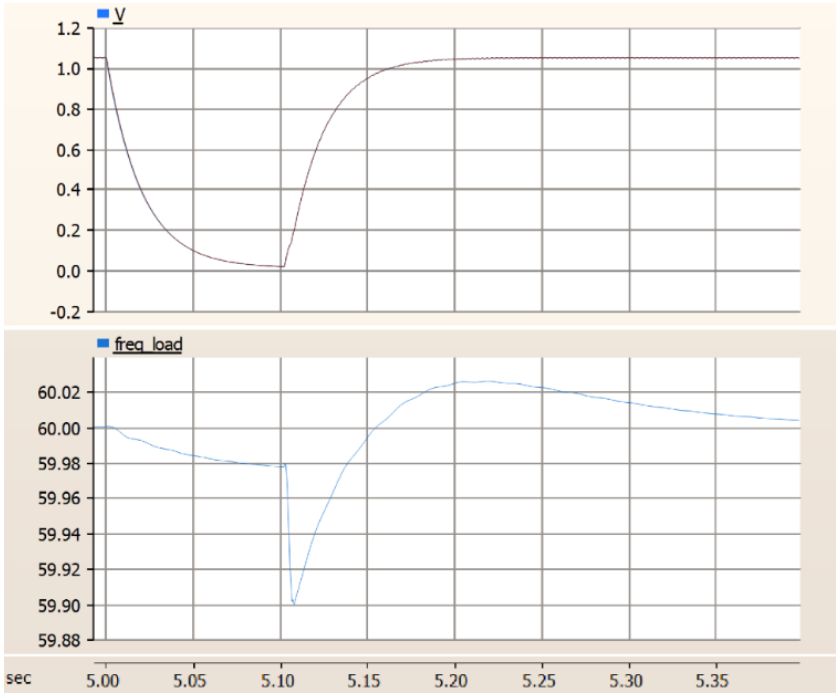

Figure 26: GFM VOC simulation results from the system of the voltage and frequency near the load during the solid three-phase to ground fault for 0.1s at 5 seconds. The voltage (PU) measurements at each bus (overlapped). The frequency (Hz) results from measurements at bus 2.